	Magnetic Calibration Boom Instrumentation Report and Results	Doc: CH-GFZ-TR-2602 Issue: 1.1 Date: 23.5.2000 Page: 1 of 43
---	---	---


CH-GFZ-TR-2602

**Magnetic Calibration of the
CHAMP Boom Instrumentation
Report and Results**

	Name	Date and Signature
Prepared by:	H. Lühr, M. Rother, R. Bock (GFZ)	<i>H. Lühr, M. Rother, R. Bock</i>
Checked by:	P. Brauer (DTU-IAU)	
Project Management:	Prof. Dr. Ch. Reigber (GFZ)	<i>Ch. Reigber 20/6/00</i>

Document Change Record

Issue	Date	Page	Description of Change
1.0	15.02.99	all	First Issue
1.1	23.5.00	13, 14, 26, 28, 33, 38,))) minor corrections

	Magnetic Calibration Boom Instrumentation Report and Results	Doc: CH-GFZ-TR-2602 Issue: 1.1 Date: 23.5.2000 Page: 3 of 43
---	---	---

ABSTRACT

This report comprises the calibration results of the CHAMP magnetometry instruments. The measurements were performed at the magnetic field facility (MFSA) of the IABG. Since CHAMP is intended to be a reference mission, the requirements in calibration quality are very high. In several cases the limitations of the MFSA had to be taken into account. As a by-product of this challenging test suggestions for improvements of the MFSA emerged.

Some major results of the calibration are:

- The scalar calibration procedure, foreseen for use in flight, was compared with the three-tilt vector method and found to be reliable.
- The scale factors of the FGMs could be determined with an uncertainty of $\pm 2 \cdot 10^{-6}$.
- The non-linearity coefficients were determined and found to be constant since May 1998.
- The angles between the CSC sensor components proved to be very stable. No change within the uncertainty band of $\pm 2''$ could be detected since their first determination in March 1998.
- The noise level of the FGMs was found to amount to some 35 pT. This provides a resolution of the measurements to one part in a million (1 ppm).
- The frequency response of the magnetometers was found to be consistent with the specifications. Measurement delay times both for the OVM and the FGMs could be determined with an uncertainty of ± 2 ms.
- The cross-talk among the two CSC sensors and the effect on the OVM measurements are as predicted. There is no influence from the OVM onto the FGMs.
- Magnetic disturbances caused by the star cameras on the boom are not detectable at the OVM, insignificant at FGM1 and of the order of 1 nT at FGM2.

This test confirmed the outstanding performance of the CHAMP boom instrumentation. Such a dedicated and well balanced magnetometry package is a good basis for a successful mission.



 <p style="text-align: center;">GFZ Potsdam</p> <p style="text-align: center;">CHAMP</p>	<p>Magnetic Calibration Boom Instrumentation Report and Results</p>	<p>Doc: CH-GFZ-TR-2602</p> <p>Issue: 1.1</p> <p>Date: 23.5.2000</p> <p>Page: 4 of 43</p>
--	--	--

TABLE OF CONTENT

1	Scope	5
1.1	Test Objective	5
1.2	Test Specimen	5
1.3	Test Date and Location	5
2	Documents	5
3	Test Condition	6
3.1	Facility and Instrumentation	6
3.2	Test Conditions	6
4	Test Setup	7
5	Sequence of Test Steps	9
6	Characteristics of the Coil Facility	13
6.1	Comparison of Calibration Techniques	13
6.2	Characteristic Parameters of the Facility	14
6.3	Field Gradients in the Facility	16
6.4	Jitter of Field Settings and Noise Floor in Facility	20
7	Parameters of the Fluxgate Magnetometers FGM1 and FGM2	22
7.1	Non-Linearity of the Scale Factors	22
7.2	Preliminary Test Results	23
7.3	Cross-Talk between the Magnetometers	24
7.4	Scale Factors of FGMs	27
7.5	Offsets of the FGMs	27
7.6	Angles between the CSC Sensor Axes	27
7.7	Misalignment between CSC Sensors.....	28
7.8	Noise Level of the Magnetometers	29
8	Dynamic Behaviour of the Magnetometers	33
8.1	Frequency Response	33
8.2	Step Response.....	35
9	Interference from the Star Cameras	38
10	Summary	43

	<p style="text-align: center;">Magnetic Calibration Boom Instrumentation Report and Results</p>	<p>Doc: CH-GFZ-TR-2602 Issue: 1.1 Date: 23.5.2000 Page: 5 of 43</p>
---	--	---

1 SCOPE

This document gives a test report and contains all the test results and derived quantities obtained during the magnetic calibrations of the CHAMP boom instrumentation performed in the magnetic facility of the IABG.

1.1 Test Objective

The prime objective of this test was to calibrate the two Fluxgate Magnetometers (FGM) in flight configuration and determine the mutual effects between neighbouring instruments. Of particular interest are:

- a) The parameters characterising the FGMs
- b) The non-linearity of scale factors
- c) The noise levels
- d) The dynamic behaviour of magnetometers
- e) The cross-talk between FGMs and OVM
- f) The interferences from the star cameras.

The results obtained here will be the basis for the data evaluation of the magnetometry instrumentation.

1.2 Test Specimen

The core part of the test is the CHAMP boom optical bench equipped with its flight hardware instrumentation and in addition the Overhauser Magnetometer (OVM) flight unit. Further details are given in [RED 04].

1.3 Test Date and Location

Date: 23 - 25 September 1998

Location: Industrienanlagen-Betriebsgesellschaft mbH (IABG), Ottobrunn, Germany

Facility: Magnetfeld-Simulationsanlage (MFSA)

2 DOCUMENTS

The following documents are referred to in this report:

- [RD 01] CH-GFZ-SP-0025, issue 1.2
Overhauser Magnetometer Specification
- [RD 02] CH-GFZ-SP-0026, issue 1.2
Fluxgate Magnetometer Specification
- [RD 03] CH-GFZ-SP-0027, issue 1.2
Star Sensor Specification
- [RD 04] CH-GFZ-TR-0023, issue 1.2
CHAMP Boom Instrumentation Magnetic Calibration, Report and Procedure
- [RD 05] IABG MFSA Test Facility Description
- [RD 06] CH-GFZ-TR-2601, issue 1.1
Compact Spherical Coil Calibration, Report and Procedure
- [RD 07] CH-GFZ-TR-2501, issue 1.1
Overhauser Magnetometer Performance Test Report

3 TEST CONDITION

3.1 Facility and Instrumentation

The calibration was performed in the magnetic test facility (MFSA) of the IABG. In the centre of the system the Earth field and its variations are compensated automatically. Artificial fields up to 80.000 nT in any direction can be generated by the coils. The field settings may either be selected manually or computer controlled. For this calibration all tests were run computer controlled using dedicated control files. The individual settings were randomly distributed to avoid a systematic heating of the coils and related errors caused by the temperature dependence of the system.

A coarse monitoring of the field settings was performed by a Förster fluxgate magnetometer placed some 4 m away from the facility centre to avoid interferences with the units under test.

The magnetometer sensors to be tested were operated by their flight electronics units (DPUs). Each DPU was controlled by its EGSE and the data were stored on the corresponding laptops. The synchronisation of the OVM and FGM measurements was assured by a common 1 Hz synchronisation pulse derived from a GPS time receiver.

3.2 Test Conditions

The temperature is a parameter which influences the characteristics of the system (e.g. thermal expansion of the coils). Even though the building is thermostated there are temperature variations of the order of ± 1 K (see Figure 3-1) which have to be taken into account when evaluating the test results.

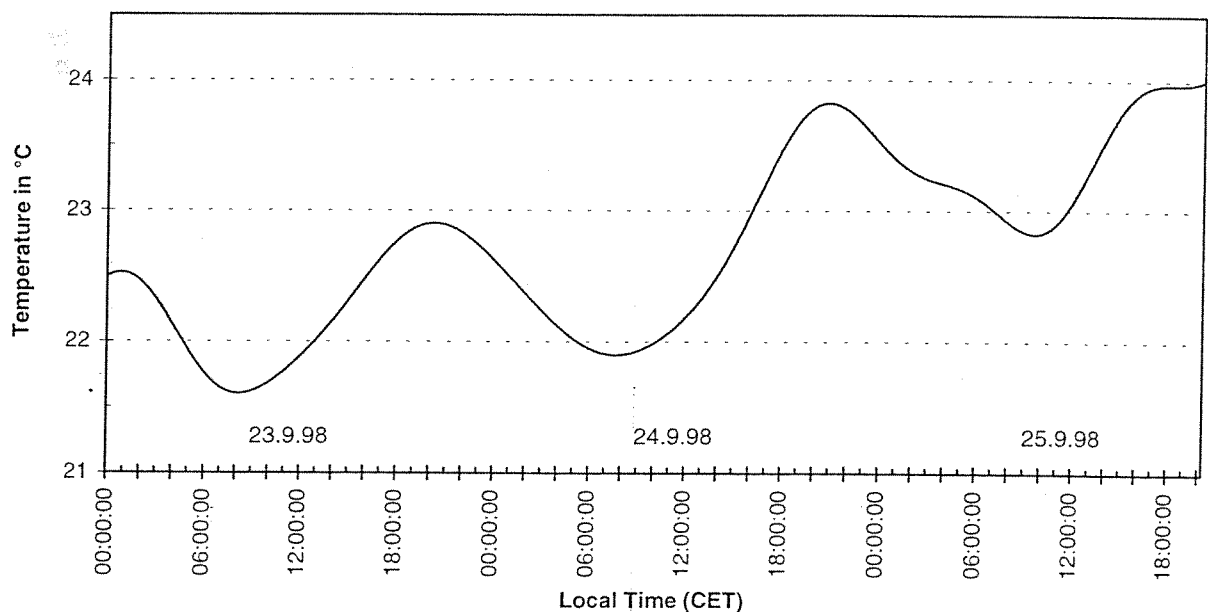


Figure 3-1 Air temperature in the MFSA during the magnetic calibration

Another relevant quantity is the geomagnetic activity which may enhance the noise floor in the system. During the first two days of the test the magnetic activity was low, as can be seen from the relevant Kp indices. A major magnetic storm commenced early 25 September. Figure 3-2 shows recordings of the three components North, West, Zenith. All crucial calibrations had been finished before the start of the storm.

YYMMDD	Kp-Index	Sum
980923	3o 3o 3- 2+ 2+ 1+ 3- 3-	20o
980924	3+ 5- 4o 4- 1+ 3- 3+ 6o	29o
980925	8- 8o 8+ 7o 6+ 6- 3- 2+	48o

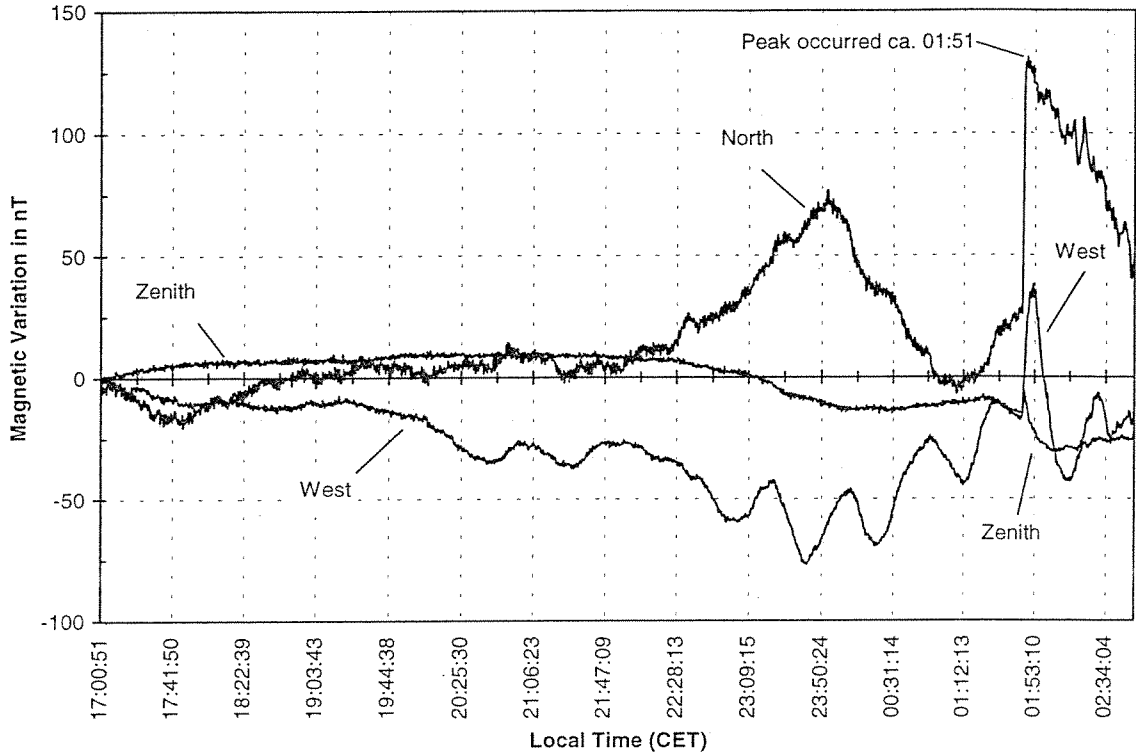


Figure 3-2 Magnetic field variations on September 24/25, 1998

4 TEST SETUP

The objective, the test setup has to fulfil, is to support a configuration of the boom instruments as close as possible to the arrangement in flight. The relative positioning of the various sensors was maintained with a precision of ± 1 mm in all axes. At the Reference Point RP1 several absolute measurements were made for determining the relevant facility parameters.

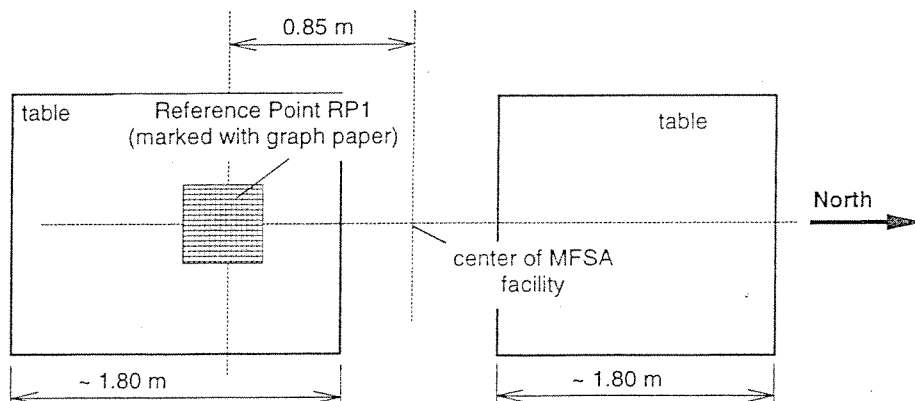


Figure 4-1 Setup for the magnetic calibration

The setup depicted in Figure 4-2, with the OVM at Reference Point RP1 and the optical bench at a proper distance, was used to calibrate the main parameters of the FGMs. For technical reasons (room for connectors) the OVM sensor had to be placed with its z axis upward. This discrepancy is of negligible influence, because of the highly omnidirectional characteristic of the OVM.

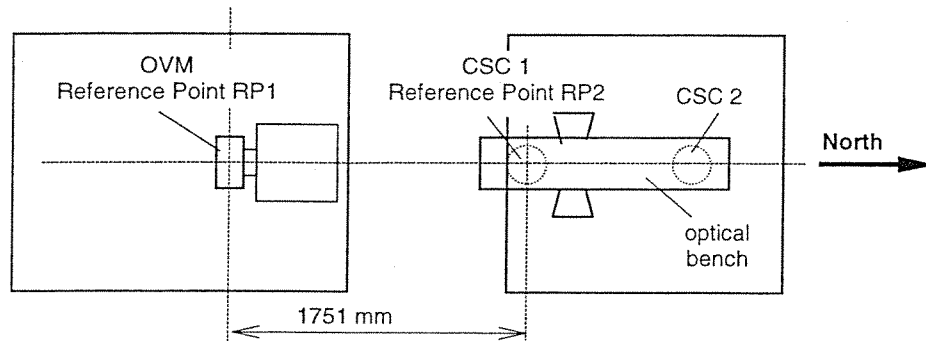


Figure 4-2 Setup with the OVM sensor at the Reference Point RP1

Coordinate assignment for Figure 4-2:

OVM		CSC 1/2	
X	South	X	South
Y	East	Y	West
Z	Zenith	Z	Nadir

The whole set of measurements performed above was repeated with the setup swapped as shown in Figure 4-3 allowing to correct for gradients in the coil system. In this configuration the FGM1 sensor,, Compact Spherical Coil CSC1, is centred at Reference Point RP1.

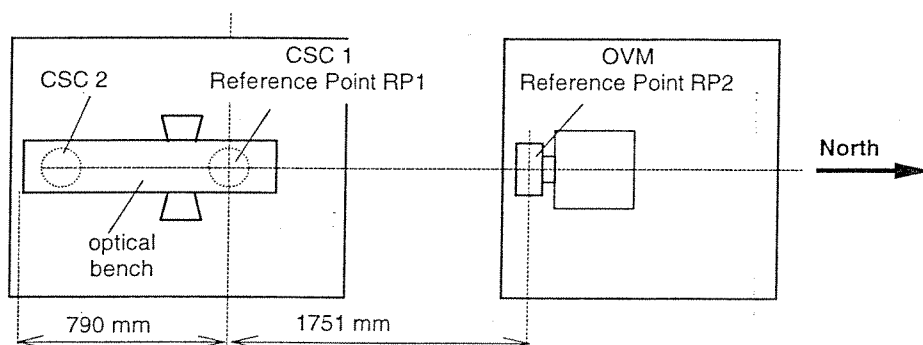


Figure 4-3 Setup with CSC1 at the Reference Point RP1

Coordinate assignment for Figure 4-3 :

OVM		CSC 1/2	
X	North	X	North
Y	West	Y	East
Z	Zenith	Z	Nadir

A last set of readings was taken with the two FGM sensors spaced equally close to the centre of the facility. The intention of this was to get another measure of the facility gradient.

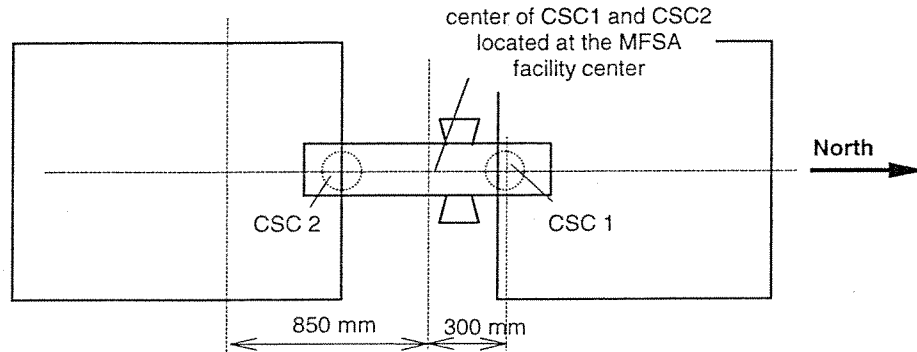


Figure 4-4 Setup for gradient field measurement

Coordinate assignment for Figure 4-4 :

CSC 1/2	
X	North
Y	East
Z	Nadir

5 SEQUENCE OF TEST STEPS

A detailed description of the step-by-step procedure is given in [RD 04]. For completeness we repeat here a condensed list with the sequence of test steps.

**Magnetic Calibration
Boom Instrumentation Report and Results
Test Steps**

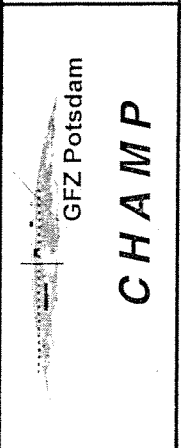
Test step	Date	Time			FileNames				Remark
		GPS	Local Time	OVM Counter	Field Settings	MFSA	FGM	OVM	
2.1	23.9.98	-	14:42	-		see printout Appendix 1	-	-	Facility calibration with GEM Adjustment of control parameters
2.21	23.9.98	305775	14:56:11	-	THIN-45.SET	thin 450	fgm3 / 23_09_98 / 12_51_00.DAT	-	Facility calibration with FGM EM
2.22	23.9.98	308455 308479	15:40:51 15:41:16	-	THIN-45.SET	thin 451	fgm3 / 23_09_98 / 13_37_00.DAT	-	Facility calibration with FGM EM
2.23	23.9.98	310804 310828 310853	16:20:00 16:20:25 16:20:50	-	THIN-50.SET	thin 452	fgm3 / 23_09_98 / 14_16_00.DAT	-	Facility calibration with FGM EM
2.3	23.9.98	-	17:09:18 17:10:07	151 200	THIN-45.SET	thin 453	-	IABG980923_01.XLS	Facility calibration with OVM
3.21	23.9.98	-	-	130 151 178 204 233 271 301	(60 μ T West)	-	-	IABG980923_02.XLS	Influence of FGM on OVM, 60 μ T West - switch-on FGM1 - switch-on FGM2 - switch-off FGM2 - switch-off FGM1 - switch-on FGM1 - switch-off FGM1
3.22	23.9.98	-	-	50 70 122 172	(60 μ T North)	-	-	IABG980923_03.XLS	Influence of FGM on OVM, 60 μ T North - switch-on FGM1 - switch-on FGM2 - switch-off FGM1 & FGM2
3.51	23.9.98	319250 319290 319350	18:40:49 18:41:27 18:42:28 18:45:43	- - - 174	LONG-50.SET	long 500	fgm1 / 23_09_98 / 16_38_00.DAT fgm2 / 23_09_98 / 16_38_00.DAT	IABG980923_4.XLS	Overnight run Setup according to Fig. 4-3 OVM lost track after 145 settings MFSA stopped after 927 settings
4	24.9.98	-	09:08	-		see printout Appendix 2	-	-	Facility calibration with GEM Adjustment of control parameters
3.31	24.9.98	-	10:02:06 10:02:56	50 100	THIN-60.SET	thin 601	-	IABG980924_02.XLS	Scalar / Vector cross calibration OVM alone
3.32	24.9.98	-	10:54:36 10:54:55 10:55:15 10:56:37 10:57:07	40 60 80 - -	THIN-60.SET	thin 602	fgm1 / 24_09_98 / 08_46_00.DAT	IABG980924_3.XLS	Scalar / Vector cross calibration OVM and FGM 1

**Magnetic Calibration
Boom Instrumentation Report and Results
Test Steps**

Doc: CH-GFZ-TR-2602
Issue: 1.1
Date: 23.05.2000
Page: 11 of 43

Test step	Date	Time			FileNames				Remark
		GPS	Local Time	OVM Counter	Field Settings	MFSA	FGM	OVM	
3.33	24.9.98	-	11:35:55 11:36:15 11:36:35	30 50 70	THIN-60.SET	thin 603	fgm1 / 24_09_98 / 09_32_00.DAT fgm2 / 24_09_98 / 09_32_00.DAT	IABG980924_4.XLS	Scalar / Vector cross calibration OVM , FGM 1 and FGM 2
3.37	24.9.98	-	11:37:27 11:38:37	-	THIN-60.SET	thin 604	-	IABG980924_05.XLS	Scalar / Vector cross calibration OVM alone Setup according to Fig. 4-3
3.38	24.9.98	-	13:54:53 13:55:13 13:55:57 13:56:27	50 70	THIN-60.SET	thin 605	fgm1 / 24_09_98 / 11_50_00.DAT	IABG980924_6.XLS	Scalar / Vector cross calibration OVM and FGM 1
3.39	24.9.98	-	14:47:30 14:47:50 14:48:27 14:49:07	50 70	THIN-60.SET	thin 606	fgm1 / 24_09_98 / 12_34_00.DAT fgm2 / 24_09_98 / 12_34_00.DAT	IABG980924_7.XLS	Scalar / Vector cross calibration OVM , FGM 1 and FGM 2 OVM lost track after ca. 26 settings
3.4	24.9.98	-	15:28:55 15:29:15 15:29:57 15:31:57	40 60	RAND-64.SET	(no data available)	fgm1 / 24_09_98 / 13_22_00.DAT fgm2 / 24_09_98 / 13_22_00.DAT	IABG980924_8.XLS	Linearity of FGMs OVM lost track after 155 settings
3.52	24.9.98	-	16:58:41 16:59:01 16:59:37 16:59:57	60 80	LONG-50.SET	long 501	fgm1 / 24_09_98 / 14_53_00.DAT fgm2 / 24_09_98 / 14_53_00.DAT	IABG980924_9.XLS	Overnight run OVM lost track after 145 settings
5.10	24.9.98	463300	(10:42)	200	(45 μ T West)	-	fgm1 / 25_09_98 / 08_36_00.DAT fgm2 / 25_09_98 / 08_36_00.DAT	IABG980925_1.XLS	Sine wave 200 mHz
5.11	25.9.98	463500		507 to 891	(45 μ T West)	-	fgm1 / 25_09_98 / 08_36_00.DAT fgm2 / 25_09_98 / 08_36_00.DAT	IABG980925_1.XLS	Sine wave 200 mHz
5.12	25.9.98	464100		1000 to 1400	(45 μ T West)	-	fgm1 / 25_09_98 / 08_36_00.DAT fgm2 / 25_09_98 / 08_36_00.DAT	IABG980925_1.XLS	Sine wave 20 mHz
(5.21)	25.9.98	464500		from 1500	(45 μ T West)	-	fgm1 / 25_09_98 / 08_36_00.DAT fgm2 / 25_09_98 / 08_36_00.DAT	IABG980925_1.XLS	Step response !! FGM data <u>not</u> compressed 50 Hz
(5.22)	25.9.98	464700		see Step (5.21)	(45 μ T West)	-	fgm1 / 25_09_98 / 08_36_00.DAT fgm2 / 25_09_98 / 08_36_00.DAT	IABG980925_1.XLS	Step response !! FGM data <u>not</u> compressed 10 Hz

Magnetic Calibration Boom Instrumentation Report and Results Test Steps



GFZ Potsdam
CHAMP

Test step	Date	Time			FileNames				Remark
		GPS	Local Time	OVM Counter	Field Settings	MFSA	FGM	OVM	
5.21	25.9.98	465650		see Step (5.21)	(45 µT West)	-	fgm1 / 25_09_98 / 08_36_00.DAT fgm2 / 25_09_98 / 08_36_00.DAT	IABG980925_1.XLS	Step response !! FGM data compressed 50 Hz
5.22	25.9.98	465300		see Step (5.21)	(45 µT West)	-	fgm1 / 25_09_98 / 08_36_00.DAT fgm2 / 25_09_98 / 08_36_00.DAT	IABG980925_1.XLS	Step response !! FGM data compressed 10 Hz
5.23	25.9.98	465000		END: 2870	(45 µT West)	-	fgm1 / 25_09_98 / 08_36_00.DAT fgm2 / 25_09_98 / 08_36_00.DAT	IABG980925_1.XLS	Step response !! FGM data 1 Hz
7.1	25.9.98	467190 467240	11:46:26 11:47:16	- -	THIN-60.SET	thin 607	fgm1 / 25_09_98 / 09_39_00.DAT fgm2 / 25_09_98 / 09_39_00.DAT	-	Gradient measurement (FGM 1 and 2) Opt. Bench approx. at centre of facility Setup according to Figure 4-4.
7.2	25.9.98	471620 471640	13:00:16 13:00:36	- -	THIN-60.SET	thin 608	fgm1 / 25_09_98 / 10_53_00.DAT	-	Measurement FGM 1 alone Opt. Bench approx. at centre of facility
7.3	25.9.98	473940 473970	13:38:56 13:39:26	- -	THIN-60.SET	thin 609	fgm2 / 25_09_98 / 11_34_00.DAT	-	Measurement FGM 2 alone Opt. Bench approx. at centre of facility
6.11	25.9.98	480391 480453	(15:30)	1160 1230	45 000 nT North	-	fgm1 / 25_09_98 / 13_24_00.DAT fgm2 / 25_09_98 / 13_24_00.DAT	IABG980925_2.XLS	1. Time value: ASC ON 2. Time value: ASC OFF CHU1 and CHU2 covered
6.12	25.9.98	480560 480625	-	1340 1403	45 000 nT North	-	fgm1 / 25_09_98 / 13_24_00.DAT fgm2 / 25_09_98 / 13_24_00.DAT	IABG980925_2.XLS	CHU2 covered
6.13	25.9.98	480700 480755	-	1475 1533	45 000 nT North	-	fgm1 / 25_09_98 / 13_24_00.DAT fgm2 / 25_09_98 / 13_24_00.DAT	IABG980925_2.XLS	CHU1 covered
6.14	25.9.98	481435 481550	-	2213 2293	45 000 nT North	-	fgm1 / 25_09_98 / 13_24_00.DAT fgm2 / 25_09_98 / 13_24_00.DAT	IABG980925_2.XLS	CHU1 covered
6.15	25.9.98	481605 481690	-	2385 2469	45 000 nT North	-	fgm1 / 25_09_98 / 13_24_00.DAT fgm2 / 25_09_98 / 13_24_00.DAT	IABG980925_2.XLS	non covered

6 CHARACTERISTICS OF THE COIL FACILITY

The features of the IABG magnetic test facility (MFSA) have been studied in great detail to make sure that limitations imposed by the facility do not contaminate the calibration parameters of the CHAMP magnetic field instruments. The instrumentation on CHAMP represents state of the art technology and the adequate calibration is therefore a rather demanding task.

6.1 Comparison of Calibration Techniques

CHAMP as a reference mission intends to measure the magnetic field with an absolute accuracy which can be traced back to the readings of a single instrument, in our case the Overhauser Magnetometer (OVM). The same OVM is used as the magnetic field standard throughout this test. The gyro-magnetic ratio used for the data evaluation is

$$\gamma_p = 23.4872038 \frac{\text{nT}}{\text{Hz}}$$

according to IAGA's recommendation [RD 07]. In order to check the precision of the frequency meter in the OVM the number of oscillations of its reference quartz occurring during a GPS-second are counted. Relevant corrections have been applied to the readings.

For determining the parameters of the coil facility three different methods were used:

1. Adjustment of the facility control parameters with the help of a GEM Overhauser magnetometer at the Reference Point RP1.
2. Check of the resulting facility parameters with the CHAMP OVM by applying a set of 82 field settings with evenly distributed directions.
3. Determination of the facility parameters with the fluxgate magnetometer (flight unit DPU; engineering model CSC) by applying the same 82 field settings three times after another but aligning each time another sensor axis with the north/south direction. This method, hereafter called 3-tilt calibration, allows to determine the facility and sensor parameters simultaneously.

Great care was taken that for all these measurements the centre of the relevant sensor matched as close as possible the position of Reference Point RP1. Resulting uncertainties are of the order of a millimetre.


Method 1 was used to make the scale factors 1, the offsets zero and angles between the coil axes 90°. This procedure was quite effective as could be shown by the subsequent OVM measurements (Method 2).

Parameters of the coil facility (OVM)	
Scale factors	$S_W = 0.9999315 \text{ nT/EU}$ $S_N = 0.9999267 \text{ nT/EU}$ $S_D = 0.9999230 \text{ nT/EU}$
Offsets	$O_W = 0.31 \text{ nT}$ $O_N = 0.56 \text{ nT}$ $O_D = 0.64 \text{ nT}$
Misalignment angles	$(W,N) = 90.0008^\circ$ $(W,D) = 90.0005^\circ$ $(N,D) = 90.0005^\circ$

where the indices W, N and D denote west-, north- and downward, respectively.

The systematic shortage of the scale factors by some 60 ppm is probably due to a lack of precise gyro-magnetic ratio and/or quartz frequency calibration within the GEM Overhauser magnetometer.

Method 3, applying the 3-tilt calibration, provided very consistent results. For the coil facility we obtained:

 <p style="text-align: center;">GFZ Potsdam</p> <p style="text-align: center;">CHAMP</p>	<p>Magnetic Calibration Boom Instrumentation Report and Results</p>	<p>Doc: CH-GFZ-TR-2602 Issue: 1.1 Date: 23.5.2000 Page: 14 of 43</p>
--	--	--

Parameters of the coil facility (3-tilt)	
Scale factors	$S_W = 0.99993355 \text{ nT/EU}$ $S_N = 0.9999267 \text{ nT/EU}$ $S_D = 0.9999208 \text{ nT/EU}$
Offsets	$O_W = 0.0 \text{ nT}$ $O_N = 0.46 \text{ nT}$ $O_D = 0.1 \text{ nT}$
Misalignment angles	$(W,N) = 90.0007^\circ$ $(W,D) = 90.0004^\circ$ $(N,D) = 90.0004^\circ$


As a by-product the parameters for the FGM EM emerged:

Parameters of the FGM EM	
Scale factors	$S_1 = 1.000268 \text{ nT/EU}$ $S_2 = 1.001417 \text{ nT/EU}$ $S_3 = 1.000171 \text{ nT/EU}$
Offsets	$O_1 = 57.3 \text{ nT}$ $O_2 = 36.5 \text{ nT}$ $O_3 = 20.6 \text{ nT}$
Misalignment angles	$(1,2) = 89.9651^\circ$ $(1,3) = 89.9631^\circ$ $(2,3) = 89.9600^\circ$

From a comparison of the results from Methods 2 and 3 it is obvious to see that the scalar calibration gives virtually the same numbers. We may take this as a proof that the scalar calibration method does not suffer from an inherent problem as it could have been concluded with regard to the calibration at the Braunschweig facility [RD 06]. The discrepancy we discovered there was probably due to a heading error of the GEM Overhauser magnetometer. The OVM sensor also exhibits a small heading error [RD 07] which was not taken into account here. Its effect causes slightly too large offsets in Method 2 by 0.03 nT, 0.18 nT, 0.14 nT in the West, North, Downward components, respectively. Considering these minor corrections will even further improve the match between Method 2 and 3.

6.2 Characteristic Parameters of the Facility

The characteristic parameters of the coil facility, scale factors, offsets and misalignments, have been repeatedly checked for all runs where the OVM was operating. Below the results of these evaluations are listed to get an idea of the stability of the facility characteristics.

 CHAMP	Magnetic Calibration Boom Instrumentation Report and Results	Doc: CH-GFZ-TR-2602
		Issue: 1.1
		Date: 23.5.2000
		Page: 15 of 43

Date	Time	Step	Temperature, °C	Position	S _w , nT/EU	S _N , nT/EU	S _D , nT/EU
23/9	17:10	2.3	22.71	RP1	0.9999315	0.9999267	0.9999230
23/9	18:45	3.51	22.87	RP1	0.9999246	0.9999204	0.9999123
24/9	10:05	3.31	22.00	RP1	0.9999390	0.9999405	0.9999453
24/9	11:00	3.32	22.09	RP1	0.9999367	0.9999391	0.9999471
24/9	11:40	3.33	22.17	RP1	0.9999339	0.9999379	0.9999458
24/9	13:15	3.37	22.42	RP2	0.9998712	0.9999509	0.9999759
24/9	14:00	3.38	22.56	RP2	0.9998639	0.9999475	0.9999705
24/9	14:50	3.39	22.74	RP2	0.9998627	0.9999432	0.9999686
24/9	15:35	3.4	22.97	RP2	0.9998532	0.9999358	0.9999607
24/9	17:00	3.52	23.36	RP2	0.9998709	0.9999389	0.9999675

Step	O _w , nT	O _N , nT	O _D , nT	(W,N)	(W,D)	(N,D)
2.3	0.31	0.56	0.64	90.0008	90.0005	90.0005
3.51	0.26	0.85	0.58	90.0008	90.0007	90.0003
3.31	-0.46	-0.42	0.79	89.9999	90.0006	89.9996
3.32	-1.17	-1.08	0.55	90.0002	90.0003	89.9998
3.33	-1.15	-1.40	0.58	90.0002	90.0001	89.9998
3.37	-0.01	0.50	0.23	89.9979	90.0005	90.0032
3.38	0.12	0.75	0.65	89.9979	90.0005	90.0031
3.39	-0.07	0.83	0.60	89.9976	90.0007	90.0029
3.4	0.11	1.22	1.26	89.9978	90.0004	90.0030
3.52	1.07	0.94	1.04	89.9976	89.9996	90.0024

For all the measurements in the upper half of the list labelled „Position R1“ the OVM was at the Reference Point RP1. While for the lower half (RP2) the position of the OVM and the Optical Bench was swapped (see Figure 4-3). It should furthermore be noted that the results have been corrected for the influence of the CSC sensors on the OVM whenever they were switched on. The relevant numbers for the cross-talk are given in Section 7.3.

When comparing the results from the various runs it is obvious that the angles between the axes are very stable. Recorded deviations are of the order of arc seconds. The offsets vary by several tenth of a nano Tesla, but their behaviour is not so important for the test.

The scale factors show variations of the order of ± 10 ppm. The main reason for that is their temperature dependence. Figure 3-1 shows the development of the air temperature during the three days of the test. Although the range of variations is rather small, significant effects are observed. As an example Figure 6-1 shows the trend in the residuals obtained from the scalar calibration of the facility during Step 3.4. We see a systematic decrease spanning some 0.4 nT. With the help of a linear regression, considering the temperature rise of 0.3 K and the applied field strength of 64000 nT we obtain a temperature coefficient of -23.4 ppm/K for the facility scale factor. For all further evaluations we have taken this temperature dependence into account. To make things better comparable all scale factors have been adjusted to 22.5°C.

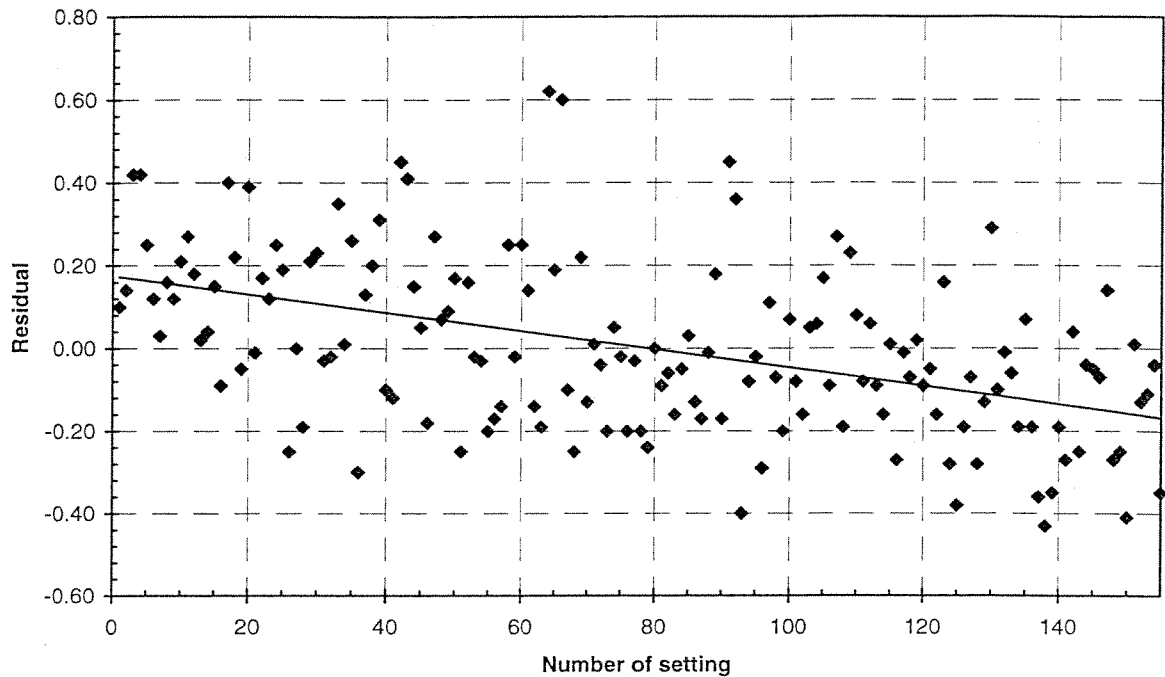


Figure 6-1 Residuals from a scalar calibration of the MFSA at 60 μT
(note the trend in the residuals caused by a temperature change)

6.3 Field Gradients in the Facility


Comparing the facility parameters obtained by the OVM at Reference Point RP1 with those at RP2 significant differences can be found. This is due to finite gradients even close to the centre of the facility. Particularly useful for the determination of these gradients are the test Steps 3.31 through 3.39. For the two locations, 1.751 m apart, we get the following temperature corrected results:

Position	S_W , nT/EU	S_N , nT/EU	S_D , nT/EU	(W,N)	(W,D)	(N,D)
RP1	0.999927	0.999930	0.999936	90.0002	90.0003	89.9998
RP2	0.999868	0.999949	0.999973	89.9978	90.0005	90.0031
RP2 - RP1	$-59 \cdot 10^{-6}$	$19 \cdot 10^{-6}$	$37 \cdot 10^{-6}$	-0.0024	0.0002	0.0033

To better visualise the effective gradients the above results and also results from the FGM measurements have been combined in Figure 6-2 and Figure 6-3. Both for the scale factors and the angles between the axes linear gradients have been estimated. The quality of the data points is not sufficient to also consider higher order terms.

Gradient of Scale Factors:

$$\frac{dS_N}{dN} = 7.4 \text{ ppm/m} \quad , \quad \frac{dS_W}{dN} = -34.3 \text{ ppm/m} \quad , \quad \frac{dS_D}{dN} = 18.7 \text{ ppm/m}$$

 <p>GFZ Potsdam CHAMP</p>	<p>Magnetic Calibration Boom Instrumentation Report and Results</p>	<p>Doc: CH-GFZ-TR-2602 Issue: 1.1 Date: 23.5.2000 Page: 17 of 43</p>
---	--	--

Gradient of the angles between axes:

$$\frac{d(W, N)}{dN} = -1.4 \cdot 10^{-3} \text{ deg/m}$$

$$\frac{d(W, D)}{dN} = 1 \cdot 10^{-4} \text{ deg/m}$$

$$\frac{d(N, D)}{dN} = 1.9 \cdot 10^{-3} \text{ deg/m}$$

Even though these numbers seem to be very small they are relevant for the evaluation of the FGM parameters when the OVM is used as the reference instrument placed at a distance of 1.75 m representing the flight configuration.

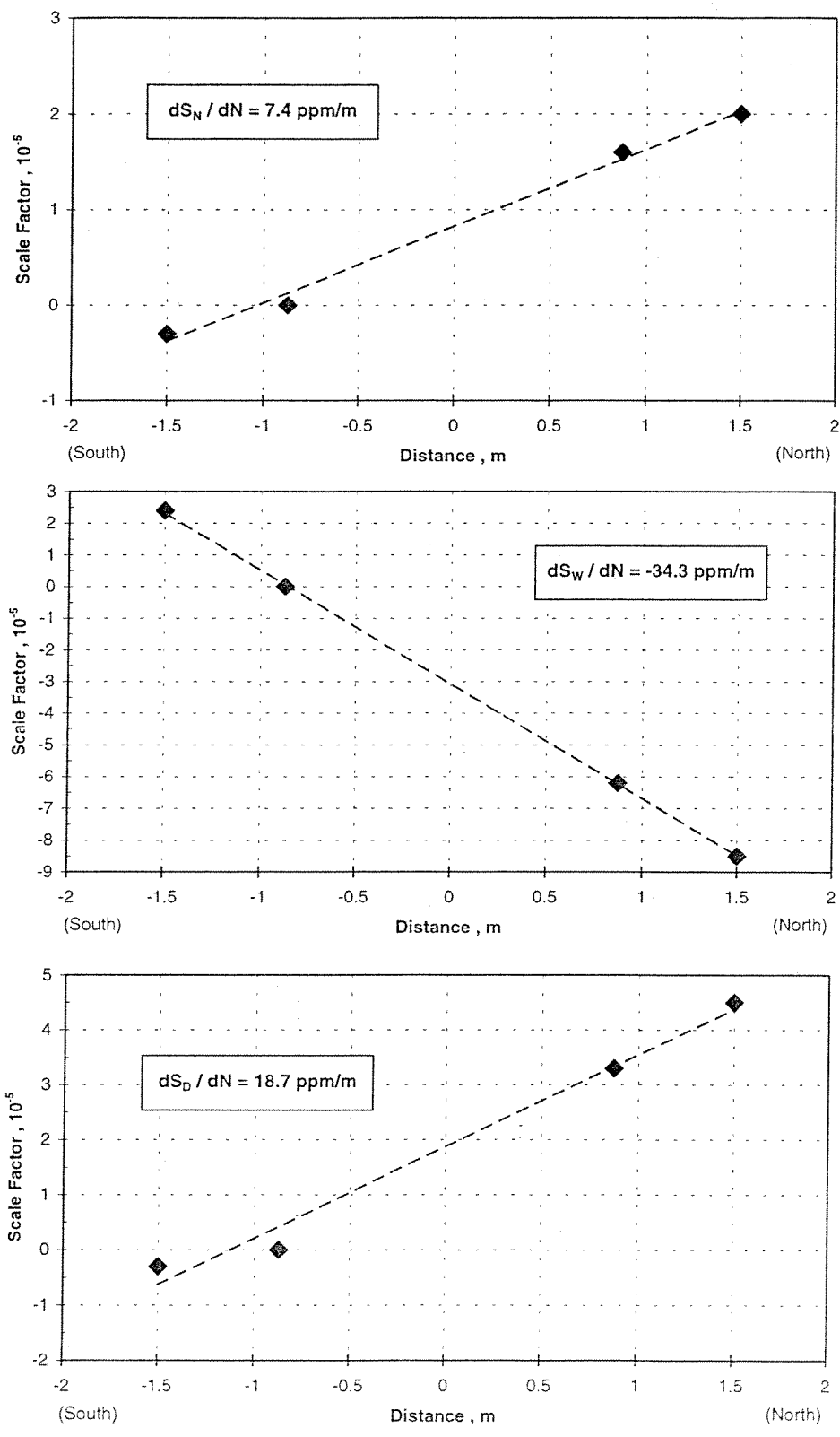


Figure 6-2 Gradients of the scale factors in the MFS

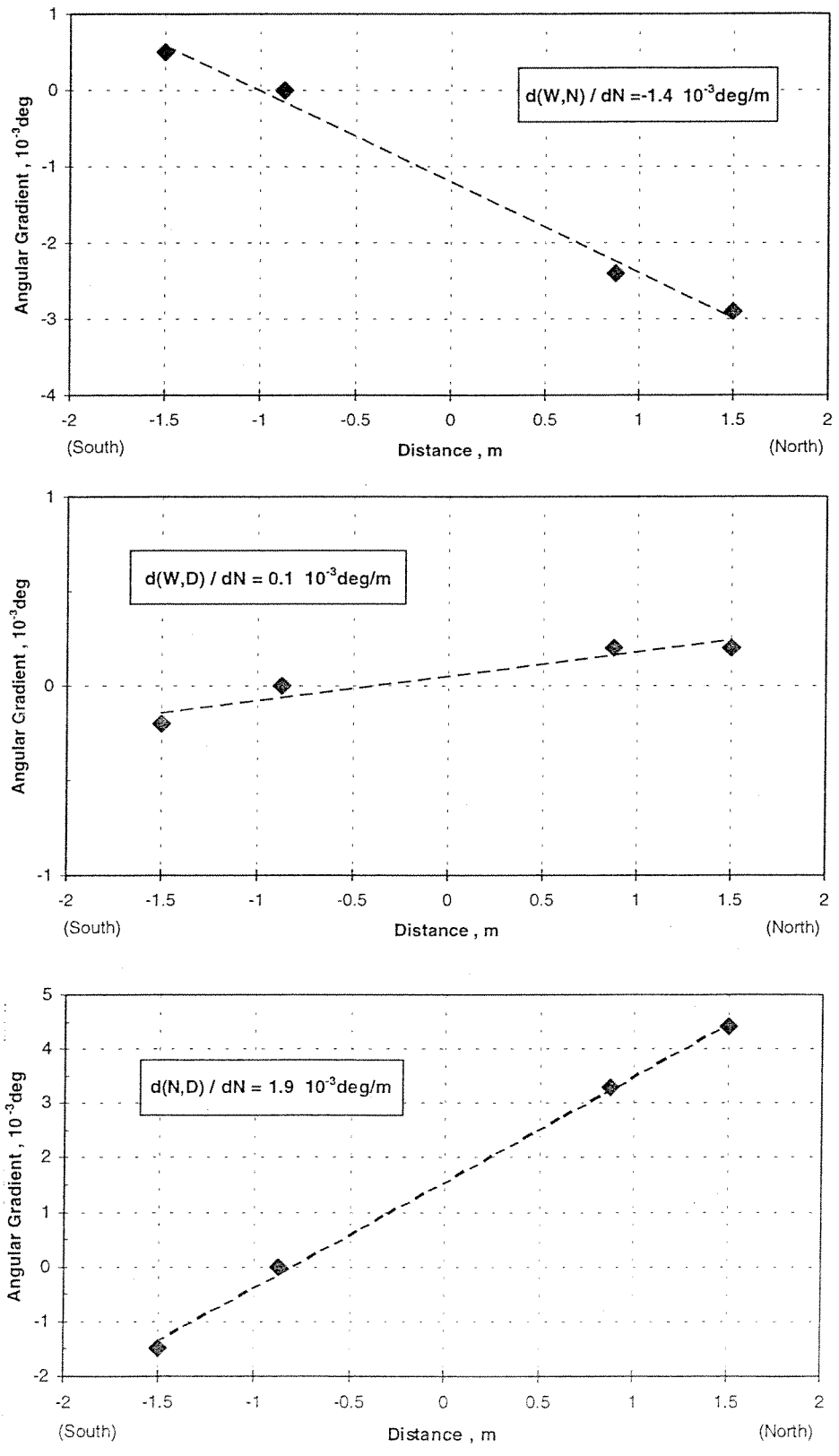


Figure 6-3 Gradients of the angles between the magnetic axes in the MFS

6.4 Jitter of Field Settings and Noise Floor in Facility

As an indicator for the quality of the applied magnetic fields we may have a look at the residuals resulting from a comparison with another magnetometer. Figure 6-4 shows as an example the residuals of Step 3.4 obtained after a comparison with the readings of FGM1. The points are spread over a band of about ± 0.5 nT in all three components. This jitter reflects the difference between the field setting and the actual output after applying all corrections mentioned in Section 6.2.

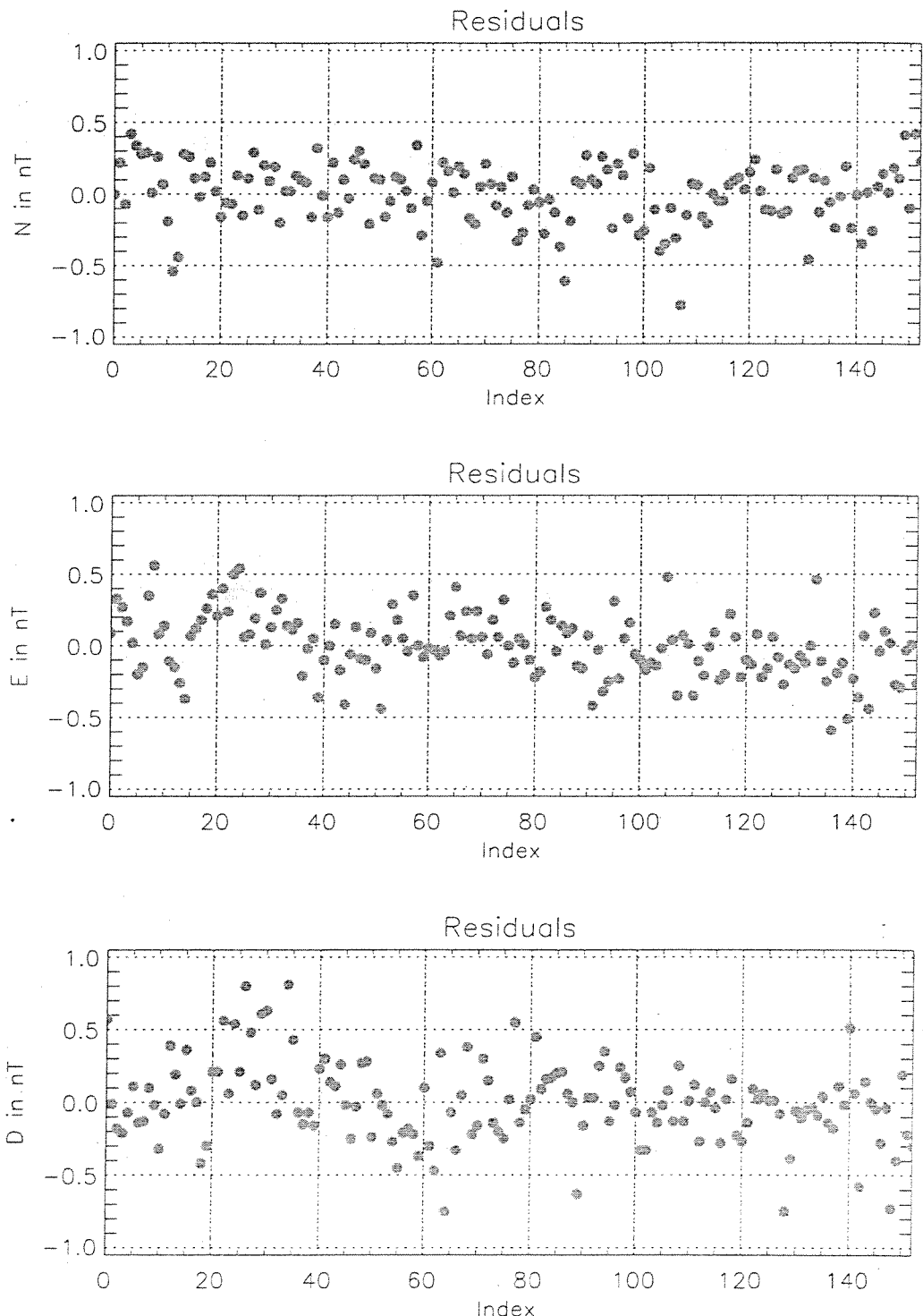


Figure 6-4 Jitter of the field settings in the three components (test Step 3.4 @ 60 μ T)

In a similar way we tried to estimate the noise floor in the facility. Figure 6-5 shows 15 min of data taken by the FGM1 at the early morning of September 24 (Step 3.51), when the ambient noise is expected to be minimal. The obtained standard deviation amounts to $\sigma = 0.18$ nT. If we have a look at the difference between the readings of the two FGMs over the same interval (see Figure 7-3) we obtain a noise level lower by a factor of 3. This result implies that Figure 6-5 really reflects the noise in the facility.

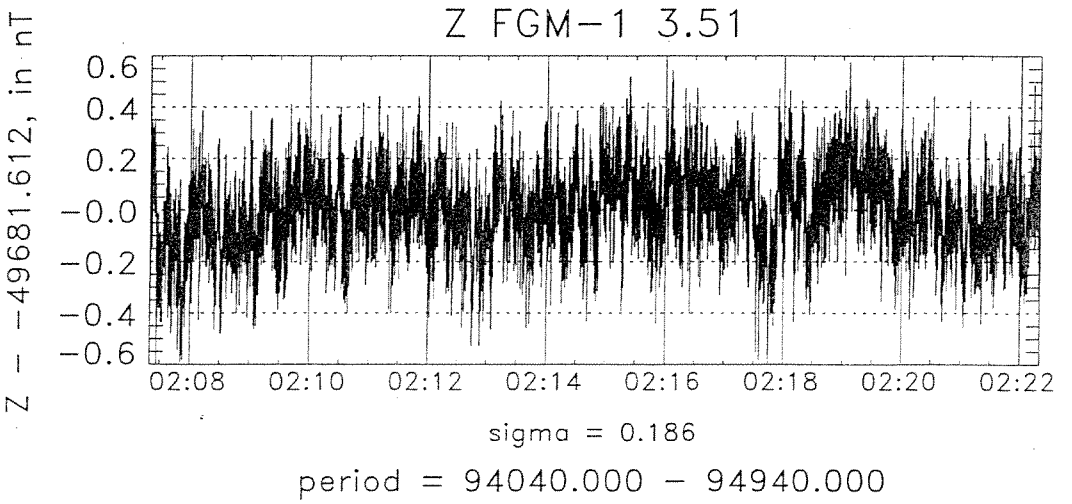
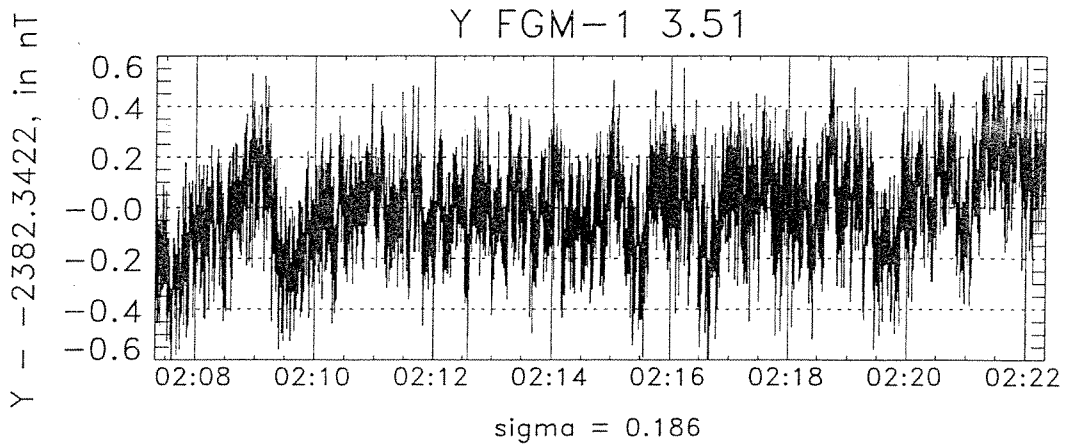
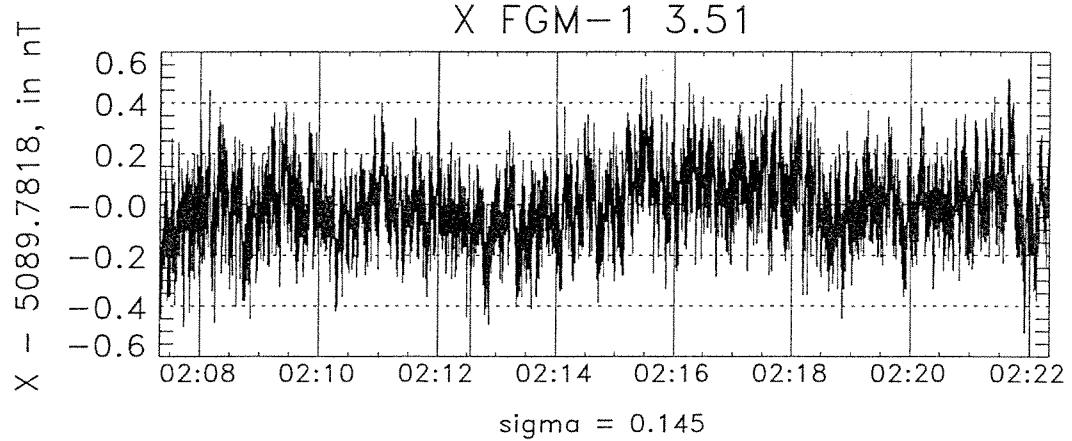


Figure 6-5 Noise floor in the MFSA measured early morning September 24, 1998

7 PARAMETERS OF THE FLUXGATE MAGNETOMETERS FGM1 AND FGM2

The prime objective of this test is the detailed determination of all relevant parameters of the two FGMs to fly on CHAMP. Special attention is paid to a realistic test setup reflecting the configuration during the mission.

7.1 Non-Linearity of the Scale Factors

From previous tests (i.e. calibration of the CSCs at Braunschweig [RD 06]) it is known that the Analogue-to-Digital Converters (ADC) exhibit some non-linear behaviour. The first step of the calibration data evaluation is thus to determine the coefficients of the correction procedure.

The non-linearity coefficients have been determined by two independent methods

1. in the laboratory, by applying a highly accurate voltage to the ADCs and comparing it to the output readings
2. from this test, by applying a randomly distributed set of field vectors to the magnetometers and comparing the FGM and OVM readings.


The first method is straight forward just fitting a third order polynomial to the data. The disadvantage is that only a fraction of the instrument is involved in the test.

Method 2 utilises a comparison between the FGM and OVM readings. The formula for computing the field magnitude from the vector measurements is expanded for all parameters influencing the result and solved in an iterative fashion for all these 15 parameters (including the non-linearity coefficients of the scale factor) by equating it to the actual OVM readings. The advantage of this method is that it can also be applied in space. A disadvantage is that possibly existing non-linear gradients in the coil facility (cf. Section 6.3) may alter the results because of the distance between OVM and the FGMs.

Below the results from the two methods are listed.

Non-linearity coefficients obtained in the lab						
Test step	Second order terms in 10^{-10}			Third order terms in 10^{-14}		
	X	Y	Z	X	Y	Z
FGM1	8.593	8.264	7.142	2.12	1.99	1.97
FGM2	7.936	10.961	9.960	1.88	2.63	2.53

FGM1 non-linearity coefficients obtained in this test						
Test step	Second order terms in 10^{-10}			Third order terms in 10^{-14}		
	X	Y	Z	X	Y	Z
3.32	7.80	7.42	6.84	1.93	1.86	2.25
3.33	8.12	7.53	6.97	1.93	1.88	2.17
3.38	7.42	7.38	6.08	2.42	1.62	1.85
3.39	7.93	7.63	7.14	2.61	1.70	1.92
3.4	7.96	7.48	6.88	2.27	2.01	1.84
	7.85 ± 0.27	7.49 ± 0.10	6.78 ± 0.41	2.23 ± 0.30	1.81 ± 0.15	2.01 ± 0.19

 CHAMP	Magnetic Calibration Boom Instrumentation Report and Results	Doc: CH-GFZ-TR-2602 Issue: 1.1 Date: 23.5.2000 Page: 23 of 43
---	---	--

FGM2 non-linearity coefficients obtained in this test						
Test step	Second order terms in 10^{-10}			Third order terms in 10^{-14}		
	X	Y	Z	X	Y	Z
3.51	7.87	10.32	9.57	1.33	2.46	2.59
3.33	6.62	10.13	9.83	1.89	2.34	2.40
3.39	7.72	10.41	9.99	2.51	1.96	2.43
3.4	6.95	10.36	9.59	2.26	2.56	2.12
3.52	7.93	10.26	9.33	2.03	2.48	2.41
	7.42 ± 0.60	10.29 ± 0.11	9.66 ± 0.26	2.00 ± 0.44	2.36 ± 0.24	2.39 ± 0.17

Comparing the results from the lab with those obtained during the magnetic test we find a good agreement (within the uncertainty limits) of the third order terms for both units. This result can be regarded as a confirmation of the two very different methods and as an indication for the stability of the non-linearity of the scale factors. The lab measurements were performed in May 1998 in preparation of the TMO test (JPL, Table Mountain Observatory, Pasadena, USA). For the second order term, on the other hand, we find a small but systematic difference. The coefficients obtained in this test are all smaller by about $5 \cdot 10^{-11}$ which corresponds to 0.125 nT in a 50.000 nT field. We cannot offer an explanation for this tiny discrepancy, but think it is real.

For all further evaluations we used a set of coefficients taking the second order terms from the magnetic test and the third from the lab measurements.


Non-linearity coefficients used for this test						
	Second order terms in 10^{-10}			Third order terms in 10^{-14}		
	X	Y	Z	X	Y	Z
FGM1	7.85	7.49	6.78	2.12	1.99	1.97
FGM2	7.42	10.29	9.66	1.88	2.63	2.53

During the CSC calibration at the Braunschweig facility [RD 06] a local non-linearity feature around 45.000 nT was detected amounting to some 0.2 nT. This feature could not be further investigated here due to the jitter of the field settings (cf. Figure 6-4). It requires dedicated measurements in the lab to further characterise this undulation.

7.2 Preliminary Test Results

For the evaluation of the FGM measurements we restricted ourselves to a comparison between the FGM and OVM readings. Such a procedure circumvents the limitations of the coil facility outlined in Section 6.4 and makes use of the same instrumentation which will be available in space. Corrections applied before the evaluation of the FGM parameters are the non-linearity and the temperature dependence of the CSCs as determined at Braunschweig [RD 06]. All results obtained have been reduced to a temperature $T_{CSC} = 23^\circ\text{C}$.

Below there are listings of the nine principle parameters characterising a fluxgate magnetometer: scale factors, offsets and angles between sensor axes.

	Magnetic Calibration Boom Instrumentation Report and Results	Doc: CH-GFZ-TR-2602
		Issue: 1.1
		Date: 23.5.2000
		Page: 24 of 43

FGM1: Preliminary sensor parameters									
Test step	Scale factor in nT/EU			Offset in nT			Angles between sensor axes		
	X	Y	Z	X	Y	Z	(X,Y)	(X,Z)	(Y,Z)
3.51	1.001778	1.002379	1.002083	26.52	22.56	20.71	89.9764	89.9347	89.9616
3.32	1.001562	1.002517	1.002228	26.07	22.50	20.65	89.9761	89.9351	89.9615
3.33	1.001779	1.002382	1.002087	26.07	22.59	20.58	89.9764	89.9349	89.9616
3.38	1.001593	1.002390	1.002293	25.82	22.56	21.38	89.9715	89.9351	89.9615
3.39	1.001809	1.002256	1.002150	25.94	22.58	21.43	89.9720	89.9347	89.9615
3.4	1.001810	1.002257	1.002149	25.94	22.47	21.44	89.9718	89.9348	89.9615
3.52	1.001812	1.002260	1.002150	26.19	22.61	21.61	89.9718	89.9348	89.9615

FGM2: Preliminary sensor parameters									
Test step	Scale factor in nT/EU			Offset in nT			Angles between sensor axes		
	X	Y	Z	X	Y	Z	(X,Y)	(X,Z)	(Y,Z)
3.51	0.9999724	1.003875	1.001234	15.14	10.72	24.48	89.9378	90.0255	89.9173
3.33	0.9999783	1.003884	1.001242	15.19	10.88	24.27	89.9378	90.0255	89.9173
3.39	1.000016	1.003709	1.001330	15.04	11.52	25.29	89.9326	90.0246	89.9179
3.4	1.000011	1.003704	1.001325	15.09	11.59	25.60	89.9324	90.0249	89.9178
3.52	1.000016	1.003708	1.001328	15.00	11.39	25.89	89.9324	90.0250	89.9178

For the correct interpretation of the computed parameters the details of the test setup have to be taken into account. The numbers above the dashed line result from measurements in the first position (cf. Figure 4-2) and those below the line from the second (cf. Figure 4-3). Here the gradients in the facility, as described in Section 6.3, have to be taken into account. Another effect is the cross-talk between the magnetometers, which will be discussed in the next chapter.

7.3 Cross-Talk between the Magnetometers

An important aspect of this test was to determine the influence of a running magnetometer on the neighbouring sensors. Dedicated tests (Steps 3.1 and 3.2) were devoted to this question. In Step 3.1 we tried to identify an interference of the OVM on the FGMs. There was no indication of any influence detected on the FGMs after switching on the OVM.

Test Step 3.2, on the other hand, confirmed the expected cross-talk of the CSC sensors onto the OVM measurements. Figures 7-1 and 7-2 show a sequence of FGM on/off switches in an ambient magnetic field of 60 μ T toward west and north, respectively. We see that the OVM readings are enhanced in case of a magnetic field perpendicular to the boom and reduced, if it is aligned with the boom. The amplitude of the jumps in Figure 7-1 has about half the size of that in Figure 7-2. The effect of FGM2 is as expected much smaller than that of FGM1 because of its greater distance to the OVM sensor. These more qualitative statements are not sufficient to design a correction algorithm for the OVM measurements. Later we will return to this point.

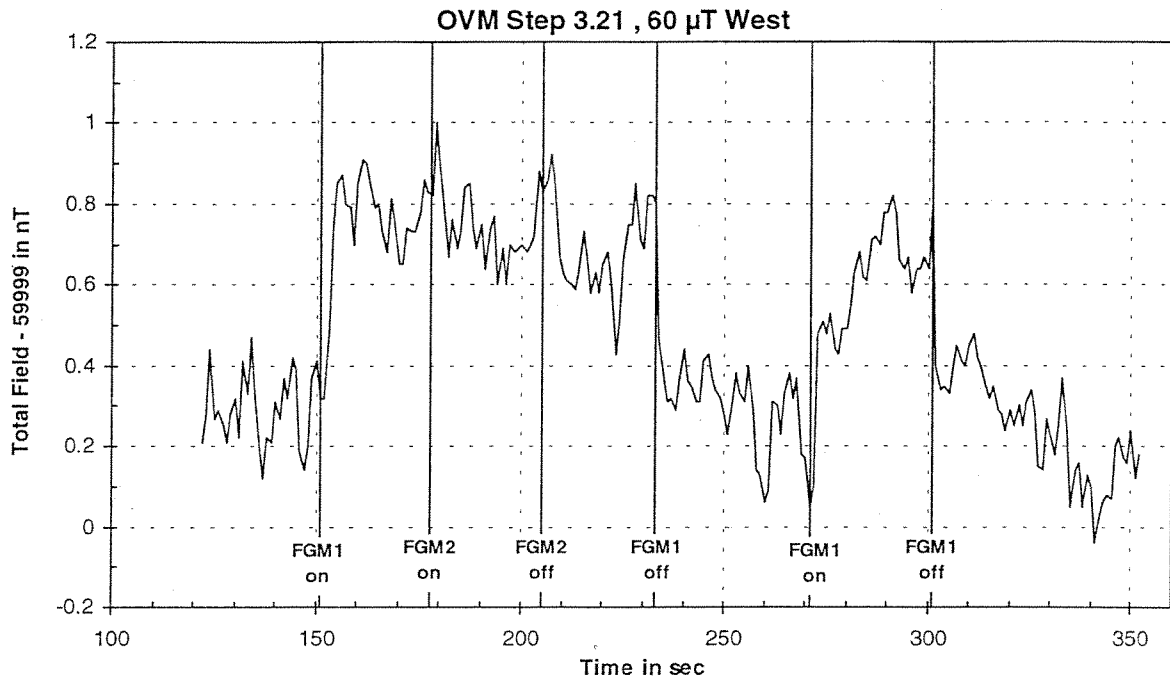


Figure 7-1 Effect of FGMs on OVM measurements in an ambient field perpendicular to the boom

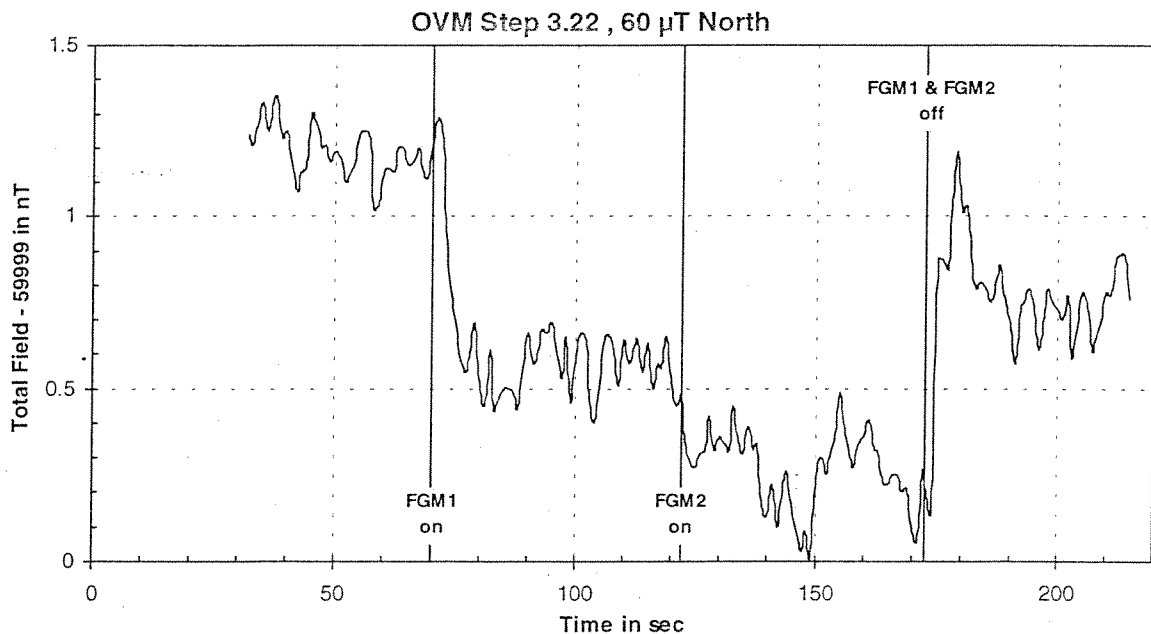


Figure 7-2 Effect of the FGMs on OVM measurements in an ambient field parallel to the boom

An even more pronounced mutual dependence exists between the two CSC sensors. The feedback windings on the spherical shell produce a dipolar field aligned with each of the measuring axes. The result is an apparent modification of the sensitivity of the neighbouring sensor. It can be written as:

$$\begin{aligned}
 S_x &= S_{xa} \left[1 - \left(\frac{R_x}{r} \right)^3 \right] \\
 S_y &= S_{ya} \left[1 + \frac{1}{2} \left(\frac{R_y}{r} \right)^3 \right] \\
 S_z &= S_{za} \left[1 + \frac{1}{2} \left(\frac{R_z}{r} \right)^3 \right]
 \end{aligned}
 \tag{7-1}$$

where S_{xa} , S_{ya} , S_{za} are the apparent sensitivities, R_x , R_y , R_z are the radii of the respective feedback windings and $r = 60$ cm is the distance between the two CSC sensors.

All measurements referred to in Section 7.2, except Steps 3.32 and 3.38, were made with both sensors operating. From the difference in scale factor of these two test steps to the adjacent measurements we can estimate the effective radii R . As a further complication it has to be taken into account, however, that the two CSCs also have a small impact on the OVM readings (cf. Figures 7-1 and 7-2). When considering all that the obtained correction factors for the CSC amount to

$$S_x = S_{xa} (1 - 2.12 \cdot 10^{-4}) \quad , \quad S_y = S_{ya} (1 + 1.35 \cdot 10^{-4}) \quad , \quad S_z = S_{za} (1 + 1.48 \cdot 10^{-4})
 \tag{7-2}$$

With the help of these factors we compute the radii

$$R_x = 3.62 \text{ cm} \quad , \quad R_y = 3.88 \text{ cm} \quad , \quad R_z = 4.00 \text{ cm}
 \tag{7-3}$$

The obtained dimensions agree within a fraction of a millimetre with the theoretical values which nicely confirms the results.

The modification of the OVM measurements by the CSC sensors can be correct for in the following way

$$B = B_{\text{OVM}} + (X^2 dx - Y^2 dy - Z^2 dz) B_{\text{OVM}}
 \tag{7-4}$$

where X , Y , Z are vector components of the ambient field, and dx , dy , dz are factors representing the influence of the CSCs. By applying the above determined dimensions of the feedback coils we get for the factors

	dx	dy	dz
CSC1 on	$8.84 \cdot 10^{-6}$	$5.44 \cdot 10^{-6}$	$5.9 \cdot 10^{-6}$
CSC2 on	$3.65 \cdot 10^{-6}$	$2.25 \cdot 10^{-6}$	$2.4 \cdot 10^{-6}$
CSC1+2 on	$12.5 \cdot 10^{-6}$	$7.7 \cdot 10^{-6}$	$8.3 \cdot 10^{-6}$

This small (~ 0.5 nT) but well determined modification of the OVM measurements will be taken into account during the satellite data processing.

7.4 Scale Factors of FGMs

After we have identified the cross-talk between the magnetometer sensors, we can start to determine the actual scale factors of the FGMs. With respect to the above listed preliminary parameters (cf. Section 7.2) there is another complication. The OVM measurements, on which the preliminary results are based, were taken at a distance of 1.75 m and 2.35 m for the FGM1 and FGM2 sensors, respectively. For this reason the gradient shown in Figure 6-2 has to be taken into account. There are two possible ways to overcome this problem (1) we take the obtained sensitivity and correct it by the gradient determined in Section 6.3, (2) we take the mean value of the scale factors obtained at the two test setups (cf. Figure 4-2 and 4-3). The second alternative has been preferred because it considers only the less noisy FGM and OVM data.

Scale factors of FGM1 in nT/EU at 23°C			
CSC 2	X	Y	Z
off	1.001594	1.002454	1.002263
on	1.001814	1.002319	1.002115

Scale factors of FGM2 in nT/EU at 23°C			
CSC 1	X	Y	Z
off	0.999794	1.003928	1.001429
on	1.000014	1.003793	1.001281

The uncertainty determined from the reproducibility of the results and from comparison between Method 1 and 2 amounts to 2 ppm and 3 ppm for the magnetometers FGM1 and FGM2, respectively.

7.5 Offsets of the FGMs

The offsets of the fluxgate magnetometers are the least stable parameters. Little effort has been put into a dedicated characterisation during this test. They have to be checked frequently by means of the in-flight calibration during the mission. Just for completeness mean values are listed here.

Offsets of the FGMs in nT			
	X	Y	Z
FGM1	26.1	22.5	21.0
FGM2	15.1	11.2	24.9

7.6 Angles between the CSC Sensor Axes

The third set of sensor parameters are the angles between the three components. Here again a careful consideration of the gradients between the reference instrument OVM and the relevant FGM is needed for a correct interpretation of the preliminary results. The angle between the (X,Y) components exhibits a significant change between the measurements in test setup 4-2 and 4-3. Opposed to that the other two pairs of angles stay more or less constant through the position change although appreciable gradients also exist in these angles (cf. Figure 6-3).

In the case of the angle (X,Y) we can simply calculate the mean (assuming a linear gradient) to obtain the actual value. This procedure does not work for the other two pairs of angles, since the gradient modifies the angles in the same direction in both positions. We used the gradients and distances of Figure 6-3 to obtain the actual values for these two angles.

Angles of the CSC sensor axes at 23°C			
	(X,Y)	(X,Z)	(Y,Z)
FGM1	89.9741	89.9381	89.9614
FGM2	89.9351	90.0299	89.9172

The uncertainty introduced by this method of gradient correction is considered to be of the order of ± 2 arcsec.

7.7 Misalignment between CSC Sensors

The components of the two FGMs are in principle aligned with the CHAMP spacecraft coordinates,

X: parallel to the boom in flight direction,

Z: downward, pointing nadir during nominal operation,

Y completes the right handed triad. In reality both sensors are slightly skewed with respect to the spacecraft system and to each other. The misalignment between the CSCs and the spacecraft system can only be determined from in-flight data, because the final orientation of the boom is hard to predict. The angles between the two CSCs are, however, assessable from the performed measurements.

The procedure use is the following: the FGM1 readings are corrected for scale factors and offsets and then transformed into an orthogonal pseudo sensor CSC1'. This pseudo sensor has the x axis in common with CSC1 and also the x-y plane is the same for both. Now the measurements of CSC2 are decomposed in the orthogonal CSC1' frame. This allows to determine the orientation of each CSC2 component in the CSC1' frame. If we assign the components of CSC1' with X1, Y1, Z1 and those of CSC2 with S1, S2, S3 we get the following matrix

	S1	S2	S3
X1	0.5164°	89.4220°	90.0835°
Y1	90.5138°	0.7024°	90.3158°
Z1	89.9479°	89.6009°	0.3267°

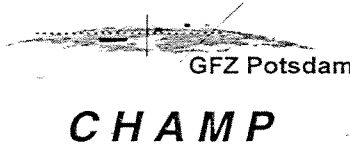
If we now define a pseudo sensor CSC2' in the same way as CSC1', we get the following orientation matrix where X2, Y2, Z2 assign the components of CSC2'.

	X2	Y2	Z2
X1	0.5188°	89.4866°	90.0557°
Y1	90.5138°	0.6482°	90.3986°
Z1	89.9479°	89.6009°	0.4051°

With the help of a 1-2-3 rotation we can transform CSC2' into CSC1'. The associated Euler angles are:

$$\varphi = -0.3991^\circ \quad \theta = 0.0521^\circ \quad \Psi = 0.5138^\circ$$

In comparison with the results obtained during the stars sensor / FGM inter-calibration at the Table Mountain Observatory (TMO), we find that these angles have changed substantially in the meantime. In

	Magnetic Calibration Boom Instrumentation Report and Results	Doc: CH-GFZ-TR-2602 Issue: 1.1 Date: 23.5.2000 Page: 29 of 43
---	---	--

particular the angle φ differs by about 0.1° . Dedicated tests are required to assess the mechanical stability of the optical bench.

7.8 Noise Level of the Magnetometers

A quality limiting the resolution of an instrument is its noise floor. In Section 6.4 we have seen that the fluctuations of the field in the coil system are relatively high. If we want to find out the noise figures of the instruments, we have to compensate for the ambient variations. Our approach is to take the readings from two magnetometers and subtract them from each other. The ambient variations will be cancelled by this approach but the uncorrelated noise of the two involved instruments sustains.

As an example we take the same interval from the early morning September 24, as shown in Figure 6-5, but plot the difference between the fluxgate readings (FGM1 - FGM2). The peak to peak noise, which can be read from Figure 7-3 is limited now to ± 0.1 nT. We compute a standard deviation of about $\sigma = 60$ pT for all three components. Assuming that both instruments exhibit the same noise characteristics, we may divide this number by square root of two and obtain a noise figure of $\sigma = 35$ pT for both fluxgate magnetometers.

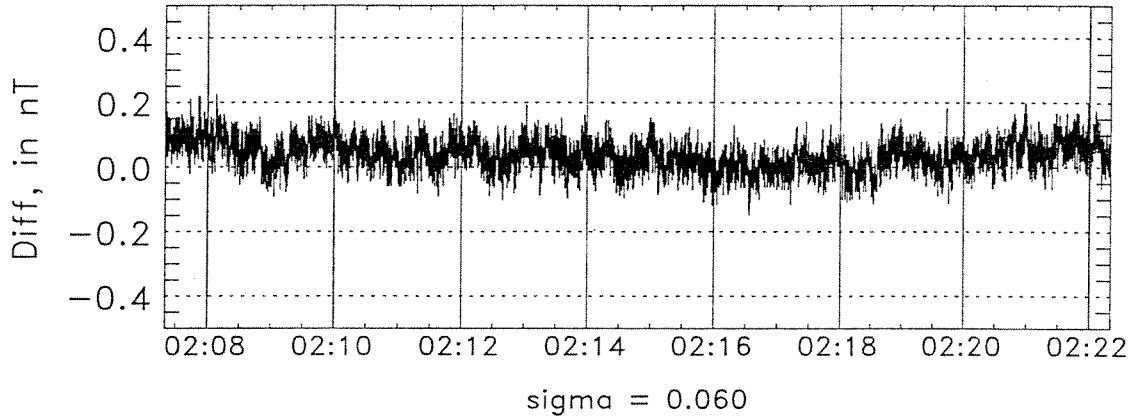
Figure 7-4 shows spectra of the noise readings. In all components the noise amplitude slopes off with one over the square root of the frequency. This behaviour is typical for fluxgate magnetometers.

We also wanted to get an idea of the variability of the field magnitude. In this case the OVM was chosen as the reference instrument. Unfortunately the OVM stopped measuring well before midnight on both days. We selected an interval of about 5 min from the beginning of Step 3.4. Figure 7-5 shows in the top panel the field magnitude computed from FGM1 in the 10 Hz mode. The standard deviation amounts to $\sigma = 0.186$ nT. The two curves in the middle panel reflect the OVM measurements (top) and the filtered and resampled FGM1 readings (bottom). The standard deviations of these two curves, reflecting essentially the variability of the coil facility, are very similar.

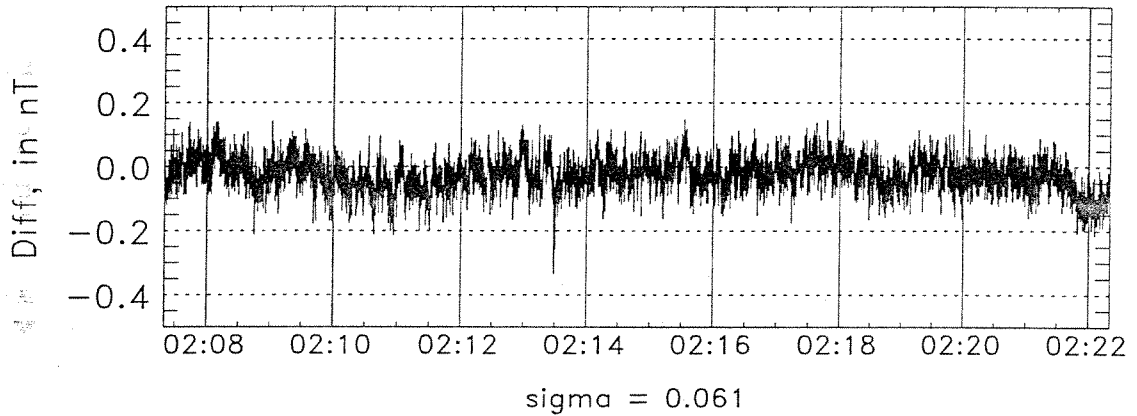
In the bottom panel of Figure 7-4 the difference of the two field magnitude measurements is plotted. The peak to peak amplitude is, except for some solitary spikes which are caused by the difference in frequency response of the two instruments, about ± 50 pT. The obtained standard deviation of $\sigma = 44$ pT is a little high but give the right order of magnitude. For the OVM we determined a noise level of 20 pT for field strengths above 40000 nT from dedicated tests [RD 07].

In summary, the FGMs were found to exhibit a noise level more than six orders of magnitudes below the full scale range. The noise figures of the two kinds of magnetometers on CHAMP (FGM and OVM) are of comparable order. This is advantageous for the common evaluation of the two data sets.

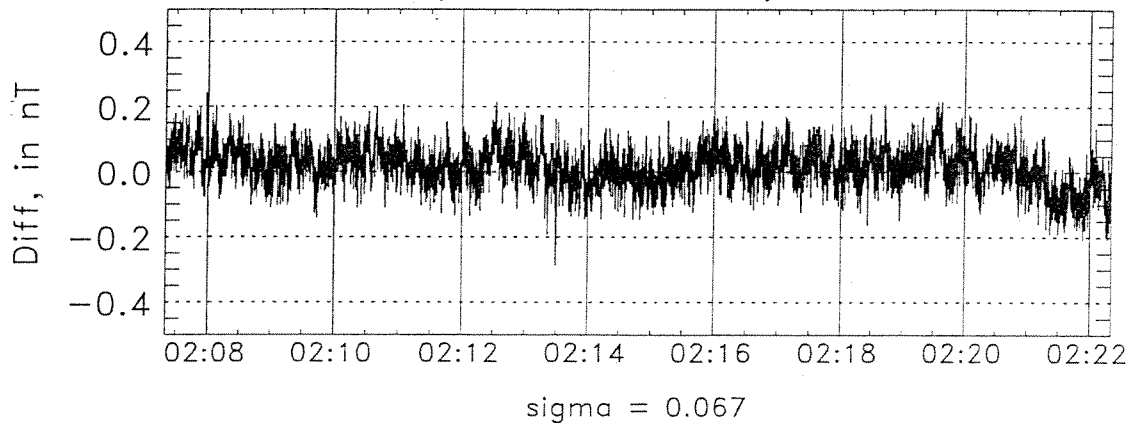
X (FGM2 - FGM1) 3.51



Y (FGM2 - FGM1) 3.51

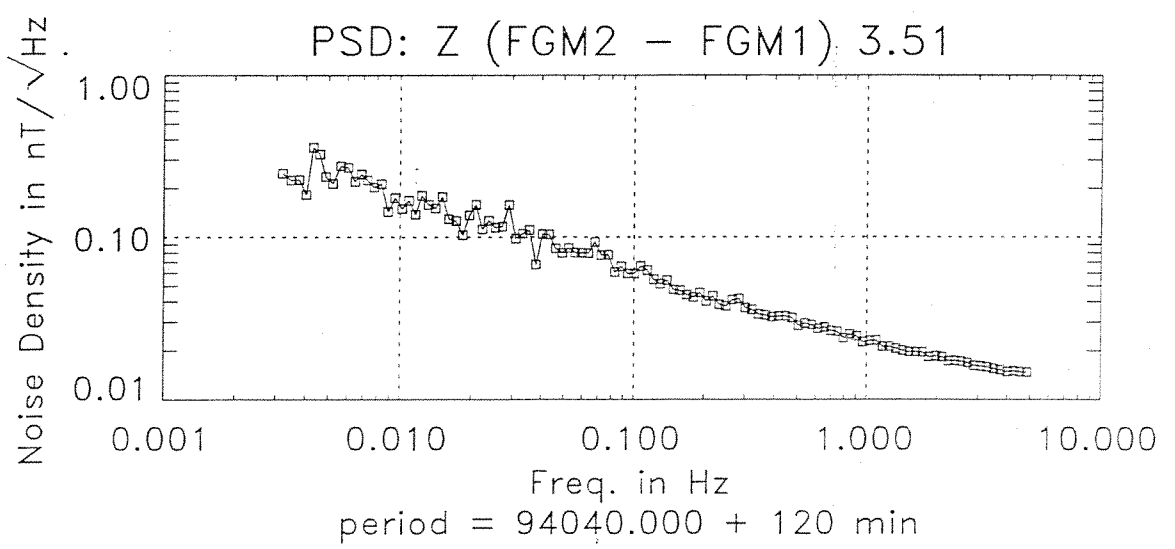
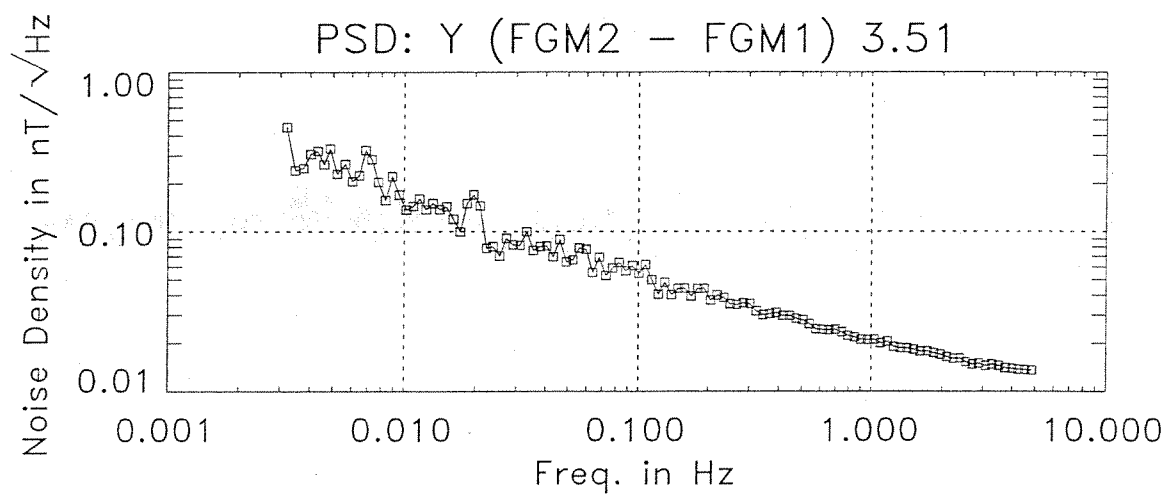
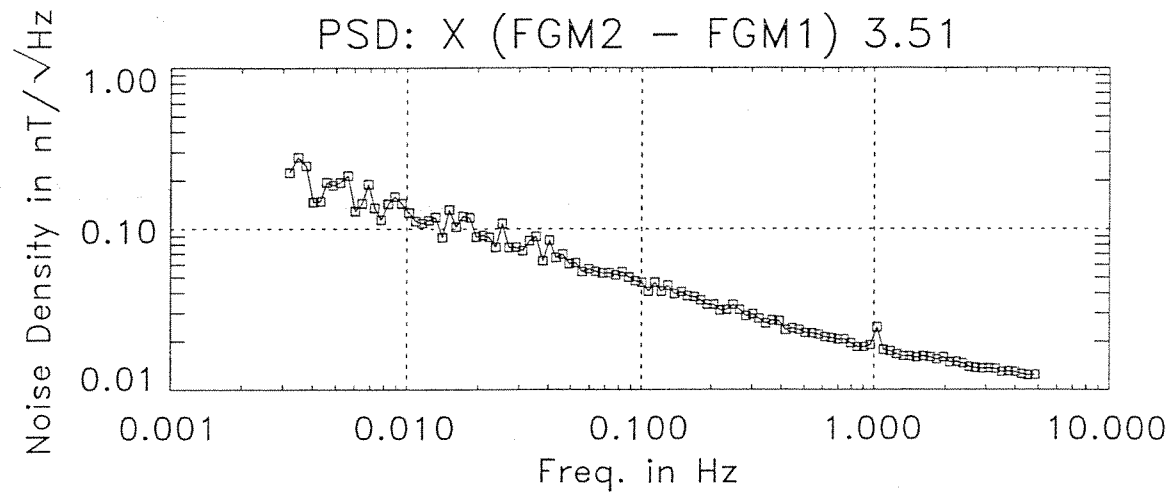


Z (FGM2 - FGM1) 3.51



period = 94040.000 + 120 min

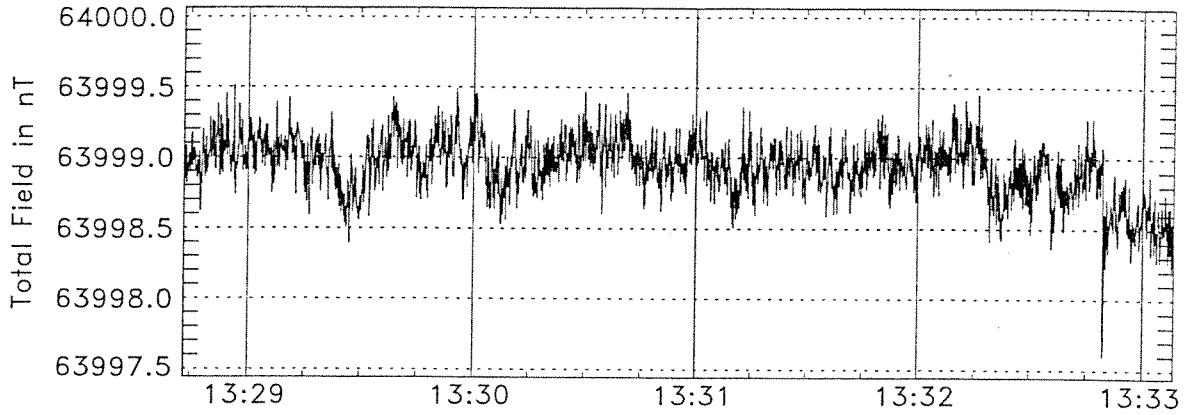
Figure 7-3 Noise level of the FGMs derived from the difference FGM 2 - FGM 1



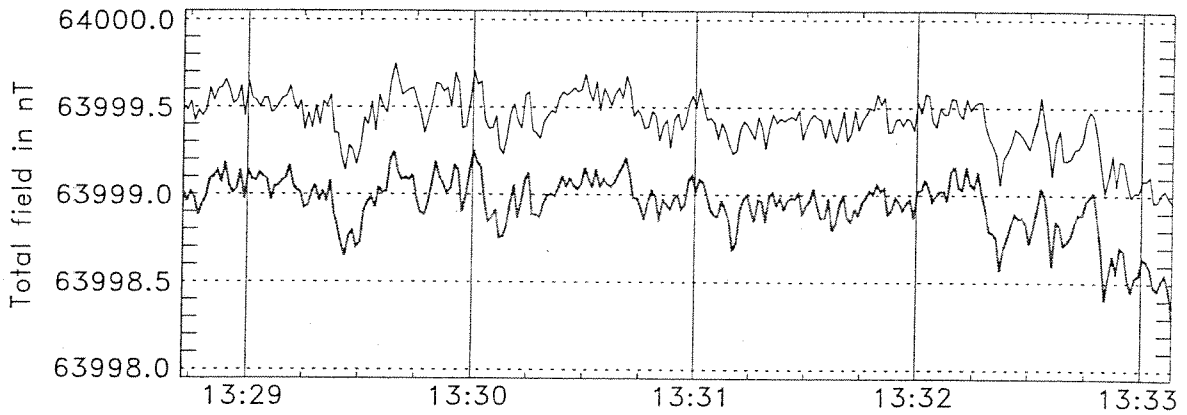
-S:\Mag\2000\ch\ch\ch\ch\Fig 10 17 51 00 1999

Figure 7-4 Spectrum of the differential noise

FGM-1 Step 3.4
 $\sigma=0.186$



OVM Step 3.4 $\sigma=0.130$
resampled FGM-1 $\sigma=0.140$



DIFF OVM - total FGM-1,
 $\sigma = 0.044$

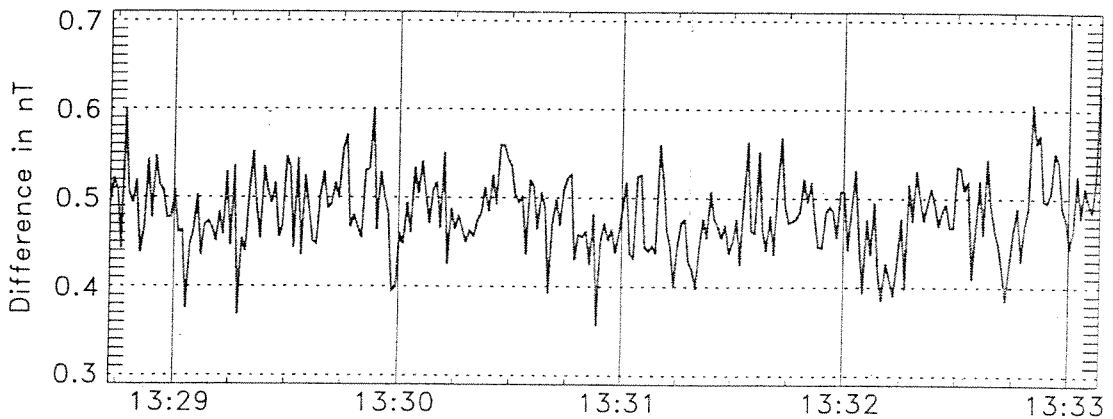


Figure 7-5 Noise of the field magnitude measurement

8 DYNAMIC BEHAVIOUR OF THE MAGNETOMETERS

The analogue outputs of the FGM components are digitised by a delta-sigma ADC which samples very often and outputs heavily filtered data. In the normal operation mode taking 50 samples per second the amplitude transfer function can be written in the form

$$A(f) = A_0 \left[\frac{\sin(2\pi f / 100)}{2\pi f / 100} \right]^3 \quad (8-1)$$

where f is the signal frequency. At frequencies of about 13 Hz we have the -3 dB cut-off.

There are further modes with 10 Hz and 1 Hz sample frequency. In these modes the data taken at 50 Hz are just averaged. This leads to an extended transfer function

$$A(f) = A_0 \left[\frac{\sin(2\pi f / 100)}{2\pi f / 100} \right]^3 \cdot \left[\frac{\sin(2\pi f / f_0)}{2\pi f / f_0} \right] \quad (8-2)$$

where f_0 is the data rate either 10 Hz or 1 Hz. The -3 dB cut-off frequencies for these latter modes are 2.2 Hz and 0.22 Hz, respectively. To give an impression of the frequency range covered we list the amplitude factors for the three modes.

Amplitude Factors			
Frequency	50 Hz	10 Hz	1 Hz
10 mH	1	1	0.9993
20 mH	1	1	0.9974
50 mH	1	0.9998	0.9836
100 mH	1	0.9993	0.9355
200 mH	1	0.9973	0.7568
500 mH	0.9995	0.9831	0
1 Hz	0.9980	0.9336	-
2 Hz	0.9921	0.7509	-
5 Hz	0.9517	0	-
10 Hz	0.8187	-	-
20 Hz	0.4335	-	-

An advantage of these filters is their linear relation between frequency and phase. Phase lags can thus be taken care of by a constant time delay, which may be part of the overall system latency.

8.1 Frequency Response

As part of the test sinusoidal signals were applied to the coil system. A sequence of 1 Hz, 0.2 Hz and 0.02 Hz waves was registered by the OVM and the two FGMs in the 50 Hz mode. Figure 8-1 gives an overview of the instruments response to the input signals. The FGMs are capable of tracking the signal very well for all three frequencies. As expected this is not the case for the OVM. At 1 Hz we find an aliased signal, at 0.2 Hz the amplitude is still markedly attenuated, and only at 0.02 Hz the OVM reproduces the input wave reasonably well.

To obtain a quantitative comparison between the recordings taken by the three instruments we applied a Fourier transform to the data sets. The time interval was in each case deliberately chosen to fit as close as possible an even number of full cycles. With this procedure we avoid leakage into higher harmonics and get a precise estimate of the frequency. The obtained results are listed below.

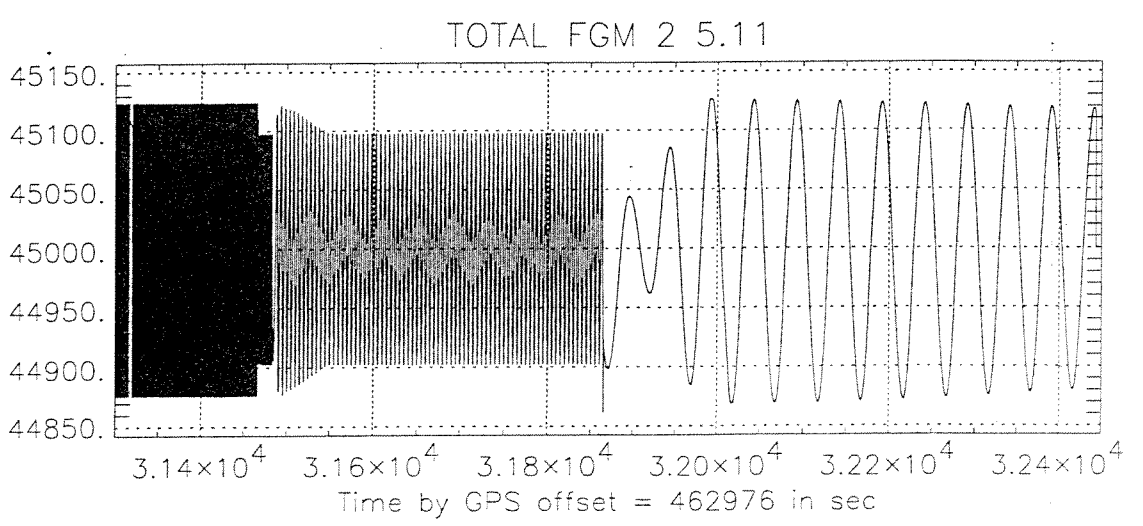
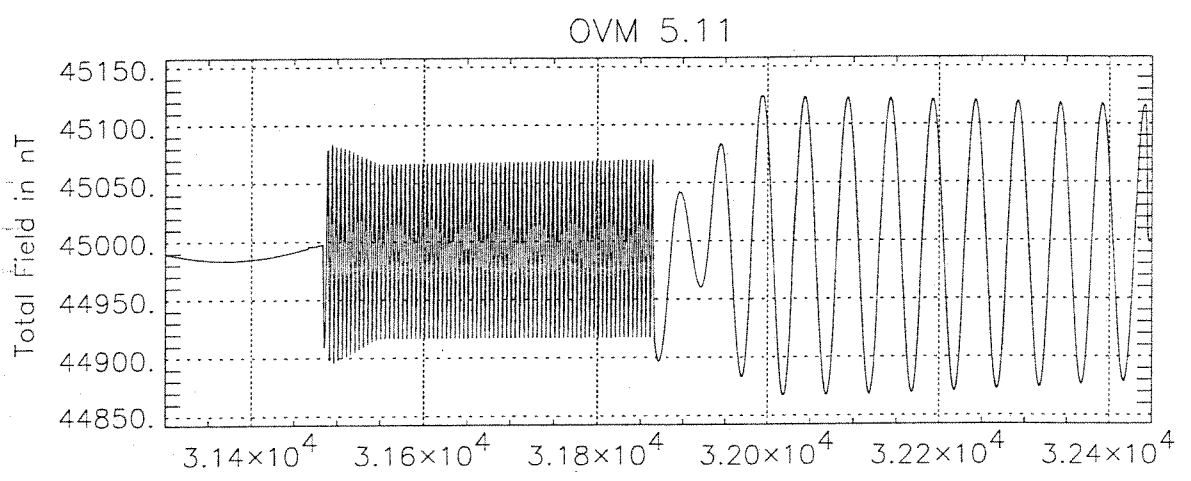
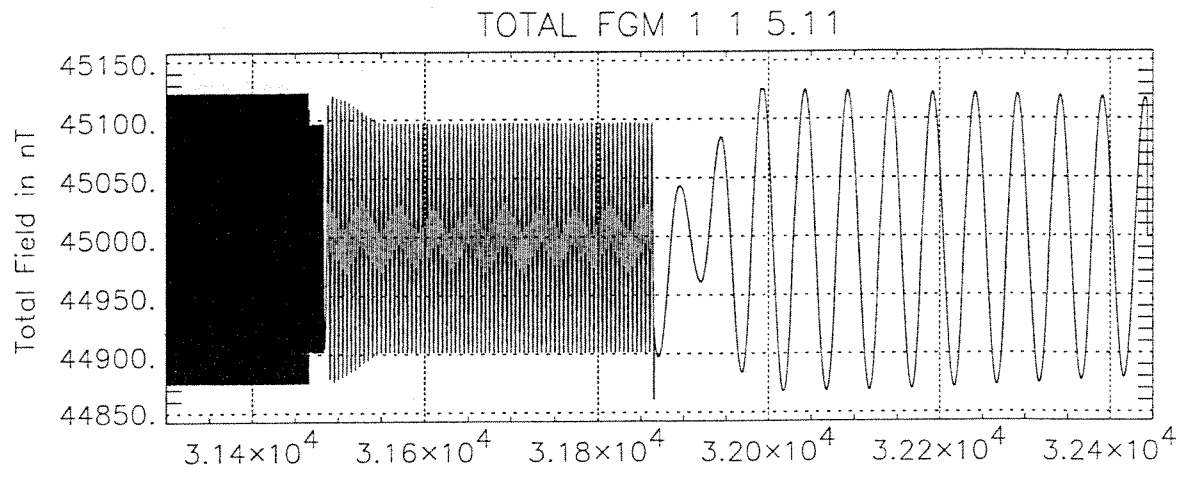


Figure 8-1 Sine wave measurements at 1 Hz, 0.2 Hz and 0.02 Hz

Instrument	Amplitude nT	Frequency mHz	Delay wrt OVM, sec	OVM / FGM ratio
OVM	14.72			
FGM1	124.11	997.86	-	0.1186
FGM2	124.10			
OVM	81.52			
FGM1	97.74	199.96	0.794	0.8340
FGM2	97.74		0.794	
OVM	124.69			
FGM1	124.87	20.06	0.831	0.9986
FGM2	124.87		0.832	

The numbers obtained for the amplitude ratio and the delay time have to be compared with the expected frequency response of the OVM as given in [RD 07]. The amplitude factor for example fits within 0.5% the expected value. The predicted delay times for the OVM are 826 and 861 ms for a 0.2 and 0.02 Hz wave, respectively. We have found delay times 32 and 30 ms shorter for the two frequencies. This means that the intrinsic delay of the FGM measurements in the 50 Hz mode is about 30 ms and there is almost no dependence on the frequency.


As a by-product of the harmonic analysis it was found that FGM2 leads FGM1 by 0.7 ms at all three frequencies. The relevance of this small difference has to be checked in separate tests.

8.2 Step Response

In the previous section we have limited our interest to harmonic signals. There will also be step-like field changes caused by switching of satellite subsystems like torquers, thrusters, valves and others. For an effective removal of these spurious signals from the data it is important to know the step response of the magnetometers.

For the OVM we have discussed the step response in great detail in [RD 07]. There is nothing new from this test that would add to our understanding of this feature. In case of the FGM we have to consider the filter characteristics given in Eq (8-1). For such filters the step response can be computed. In the 50 Hz mode we get

t, ms	b(t) immediate change	b(t) 10 ms rise time
0	0.0	0.0
5	0.016	0.008
10	0.063	0.039
15	0.156	0.109
20	0.313	0.234
25	0.500	0.406
30	0.688	0.594
35	0.844	0.766
40	0.938	0.891
45	0.984	0.961
50	1.0	0.992
55	1.0	1.0

 <p style="text-align: center;">GFZ Potsdam</p> <p style="text-align: center;">CHAMP</p>	<p>Magnetic Calibration Boom Instrumentation Report and Results</p>	<p>Doc: CH-GFZ-TR-2602 Issue: 1.1 Date: 23.5.2000 Page: 36 of 43</p>
--	--	--

It takes the FGM, as can be seen, 50 ms to fully adjust to the new level, if the signal changes abruptly. Generally there will be two readings on the ramps. For the reconstruction of the transition phase it is very important to know precisely the time of level change. In the central part the output values change by 4% per millisecond.

In several cases it is convenient to have an analytical expression approximating the step response. The above listed relative amplitude can be closely matched by the polynom

$$b(t) = 2.88 \cdot 10^{-8} (t - \tau)^5 - 4.79 \cdot 10^{-5} (t - \tau)^3 + 0.0386 (t - \tau) + 0.5 \quad (8-3)$$

where t is the time in ms and $\tau = 25$ ms is the displacement from the initiation of the step to the centre of the response curve. It has to be kept in mind here that all our considerations assume an instantaneous level change. In reality the step-like signals will have a finite slew rate which may change the shape of the response slightly.

During the test a square wave signal was fed into the coil system of the test facility. The phase relation of this signal was maintained by feeding the 1 Hz synchronisation pulse derived from a GPS clock into a counter stage. The resulting output was a 16 sec high and 16 sec low square wave with an amplitude of 30 nT.

Figure 8-2 shows the observed step response for the three sample rates of FGM1. These graphs contain useful information about the dynamic behaviour of the magnetometer. In all cases the level change took place in the second prior to the transmission of the response. The data sampled during a second are transmitted in the next. We get the most detailed picture of the response by looking at the 50 Hz sampled data. There is no response at the first point plotted at 32604.00 GPS Time (top panel of Figure 8-2). The second and third points are 8% and 69% up, respectively and the last two have already reached the new level. By comparison with the theoretical response curve we can derive the absolute timing of the individual samples. A reasonable match is obtained by affiliating 10 ms to the second, 30 ms to the third and 50 ms to the fourth sample. The apparent small discrepancy of the second point (6% predicted, 8% observed) can be explained, if we allow for a finite rise time of some 10 ms (cf. last column of above table) which is reasonable for this coil facility. All affiliated times have to be increased then by about 2.5 ms.

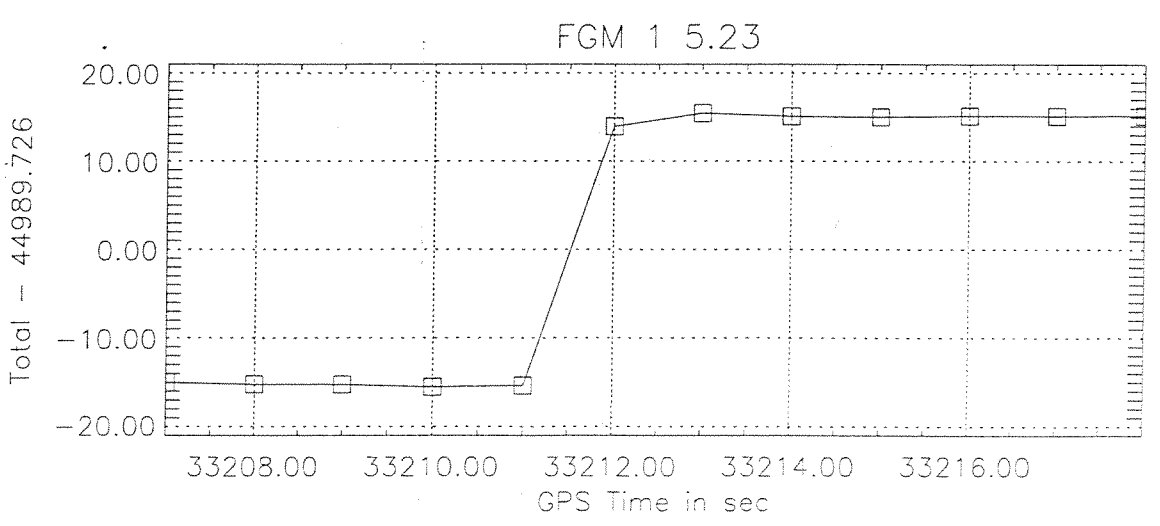
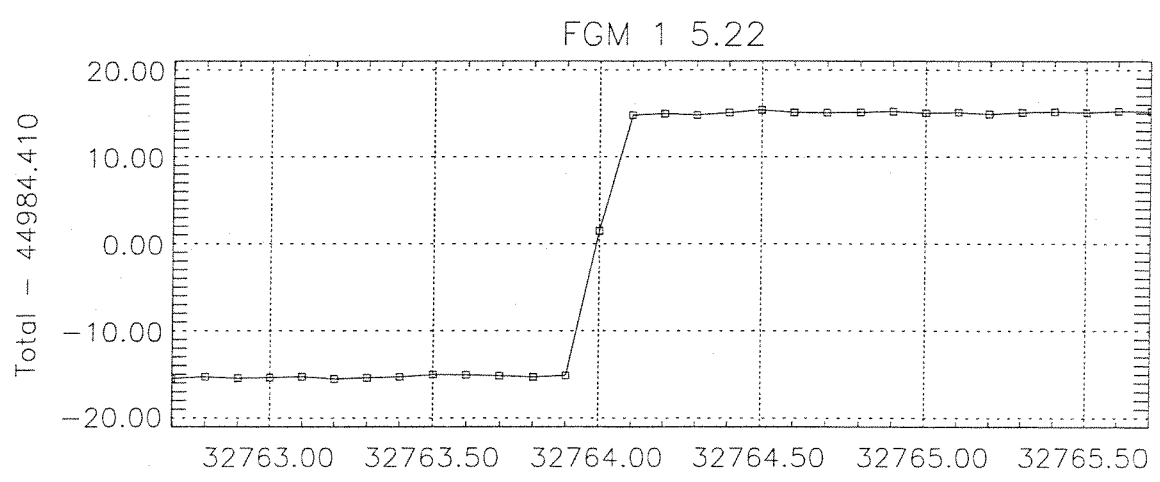
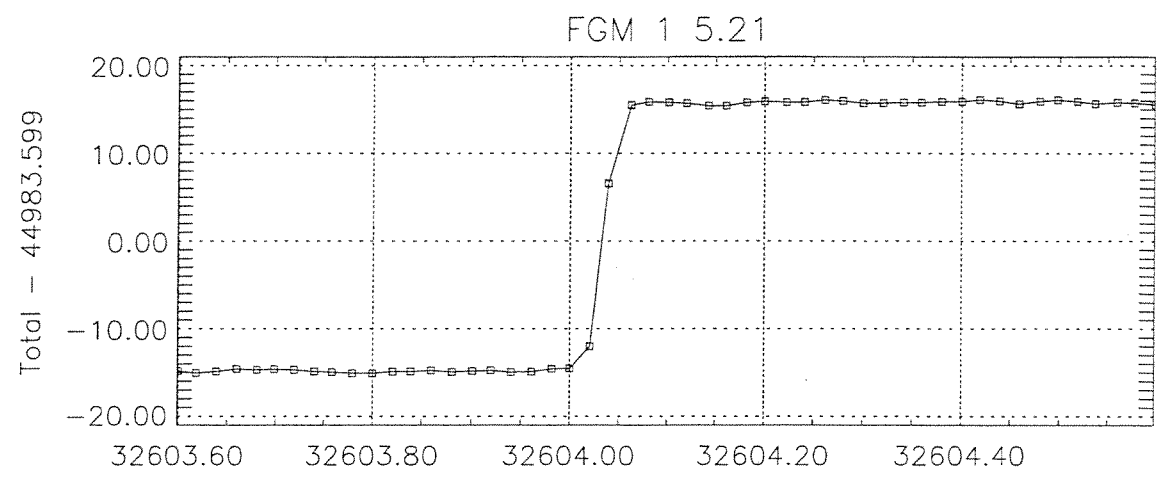
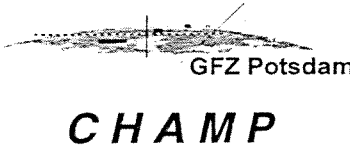


Figure 8-2 FGM step response measurements in the 50 Hz, 10 Hz and 1 Hz mode

	Magnetic Calibration Boom Instrumentation Report and Results	Doc: CH-GFZ-TR-2602 Issue: 1.1 Date: 23.5.2000 Page: 38 of 43
---	---	--

The step response in the other modes (middle and bottom panel of Figure 8-2) results just from averaging a subset of the higher sampled readings. In the 10 Hz mode we expect for the point at 32764 GPS Time the mean value of the above first five samples, 55%, which is exactly what is observed and the time affiliated to this point is 30 ms. In the 1 Hz mode we expect the sample following the step at a level of 95.5%. This is fully consistent with the observation in Figure 8-2 (bottom panel). Similarly the effective time of the sample can be set to 480 ms.

As mentioned above the primary rationale for studying the step response is the correction of step-shaped disturbances. Such an action can only be successful, if the time of occurrence of the level change is known. For the settings of the torquers a jitter of less than 5 ms is specified. From Eq (8-3) it is obvious to see that for each millisecond of mismatch between expectation and occurrence the resulting spike will grow by 4%.

In the previous chapter we derived an intrinsic delay of some 30 ms for the FGMs in the 50 Hz mode. About the same number arises from the step response. We thus can correct the phase delays independent of frequency by a constant time shift.

The relation of a given FGM reading to its actual measurement time is as follows:

50 Hz mode

$$t_{\text{Meas.}} = t_{\text{Time Stamp}} - 1035 \text{ ms} + i \cdot 20 \text{ ms} \quad ; \quad \text{where } i \text{ runs from } 0 \text{ to } 49$$

10 Hz mode

$$t_{\text{Meas.}} = t_{\text{Time Stamp}} - 995 \text{ ms} + i \cdot 100 \text{ ms} \quad ; \quad \text{for } i = 0 \text{ to } 9$$

1 Hz mode

$$t_{\text{Meas.}} = t_{\text{Time Stamp}} - 545 \text{ ms}$$

In a similar way we can describe the measurement time affiliated to an OVM reading.

$$t_{\text{Meas.}} = t_{\text{Time Stamp}} - 860 \text{ ms}$$

Although the OVM filter does not exhibit a linear phase relation with respect to frequency (cf. [RD 07]), the above equation is acceptable for all practical purposes.

9 INTERFERENCE FROM THE STAR CAMERAS

Together with the FGMs there are two star camera heads on the optical bench. The camera head units (CHU1 and CHU2) are located 20 cm in-board from FGM1 and 40 cm out-board from FGM2. The cables connecting the cameras with their electronics units run past FGM2.

In a separate test the influence of the star cameras on the magnetometers was checked. The set-up was as shown in Figure 4-3. In order to make the OVM sensitive to stray fields from the camera heads a background field of 45000 nT toward north was applied by the coil facility. Both the star cameras and the magnetometers were operated by their dedicated EGSEs.

During each test step the cameras were initially off, then on for about one minute and then off again. Magnetic fields were recorded by the three magnetometers. The considerable variability of the field in the facility (cf. Section 6.8) make it in some cases hard to discern the effect of the camera from the ambient variation. For this reason we have also considered the difference between the two FGMs, which suppresses the background noise and thus gives a much clearer picture.

The camera heads contain very light sensitive opto-electronics. Therefore they are fully saturated at normal light intensities. The following table lists the magnetic effects at the FGMs for various combinations of covered and saturated cameras.

Step	CHU1	CHU2	FGM1, nT			FGM2, nT			FGM2 - FGM1, nT		
			X	Y	Z	X	Y	Z	X	Y	Z
6.11	-	-				+0.3	-0.2	+0.4	+0.35	-0.25	+0.40
6.12	+	-				+1.3	-0.7	+0.7	+1.40	-0.55	+0.65
6.13	-	+				-0.2	-0.4	+0.1	-0.15	-0.15	+0.30
6.14	-	+				-0.2	-0.4	+0.3	-0.15	-0.25	+0.30
6.15	+	+		-0.2	-0.1	+0.7	-0.8	+0.4	+0.80	-0.55	+0.55

A minus and plus in the two left columns indicate darkened and overexposed cameras, respectively. The level of disturbance is depending significantly on the amount of light entering the cameras.

We have observed no influence of the star cameras (Advanced Stellar Compass, ASC) on the OVM measurements. Also FGM1 detected virtually no disturbances from the ASC except for some tiny deflection of about 0.2 nT when both heads are saturated (Step 6.15). Recognisable deflections are limited to FGM2. As an example Figures 9-1 through 9-3 show the effects at the FGMs for the most prominent case Step 6.12. In Figure 9-1 we see the difference between the FGM readings. This gives the clearest picture. Times of camera switch-on and off have been marked by vertical lines. Deflections of about 1 nT show up in all three components. Very much the same picture emerges from Figure 9-2 displaying the response of the FGM2 to camera switch-on. Opposed to that, no clear signature in the FGM1 measurements, as shown in Figure 9-3, can be associated with the start up of the ASC. This is surprising, since the camera heads are much closer to FGM1 than to FGM2. The only conclusion that can be drawn from this, is that the disturbances recorded at FGM2 emanate from the cables, not from the camera head electronics.

The cables of the two heads pass by FGM2 on both sides. We have tried to maximise the distance to the CSC2, but could not exceed 10 cm. The residual magnetic effect strongly depends on the configuration of individual leads in the cable. How well are the leads twisted, how well are the currents balanced between these leads? For all these reasons we cannot expect to find the same level of disturbances after the cables have been placed in their final flight position. The numbers obtained have to be regarded as qualitative estimates. The actual level of disturbances has to be determined during the system level magnetic field test at the IABG.

FGM 1→2 Step 6.12

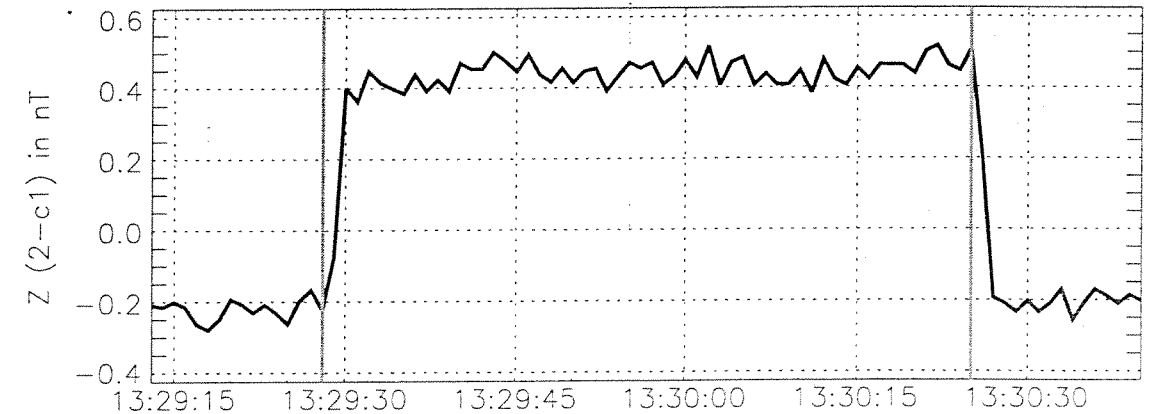
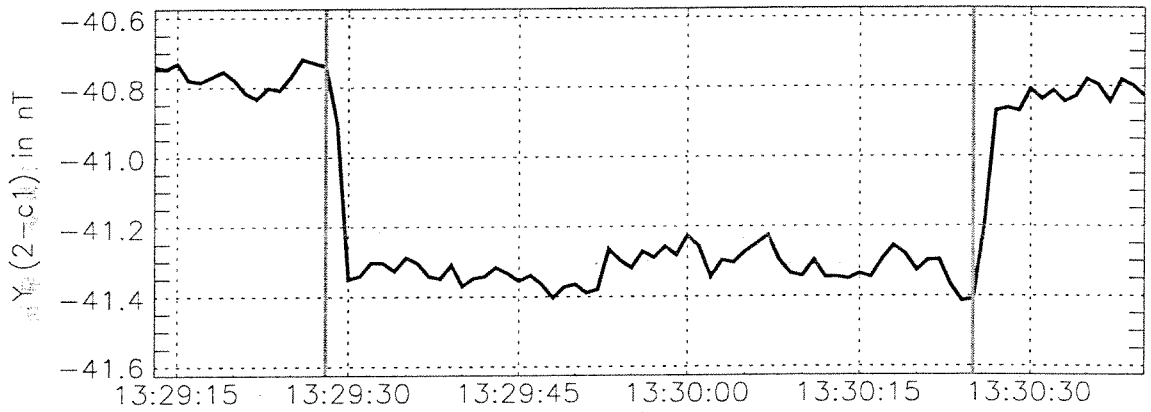
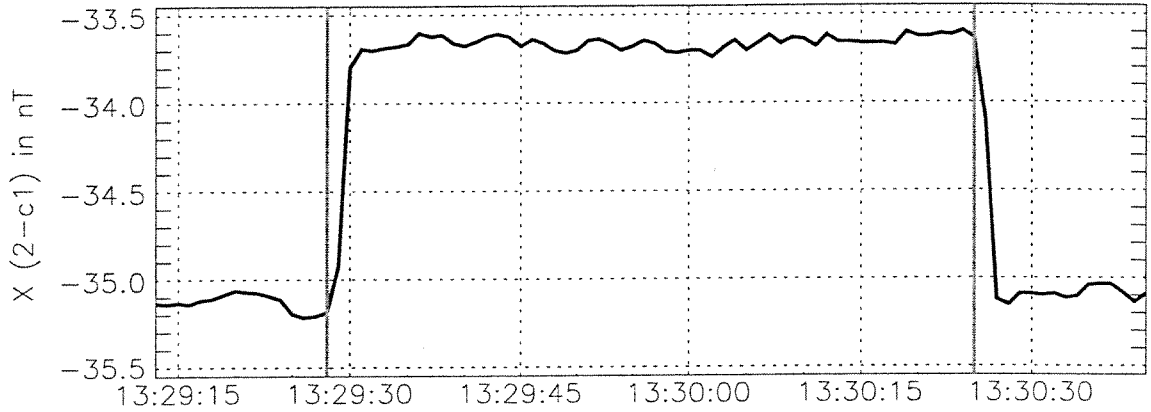
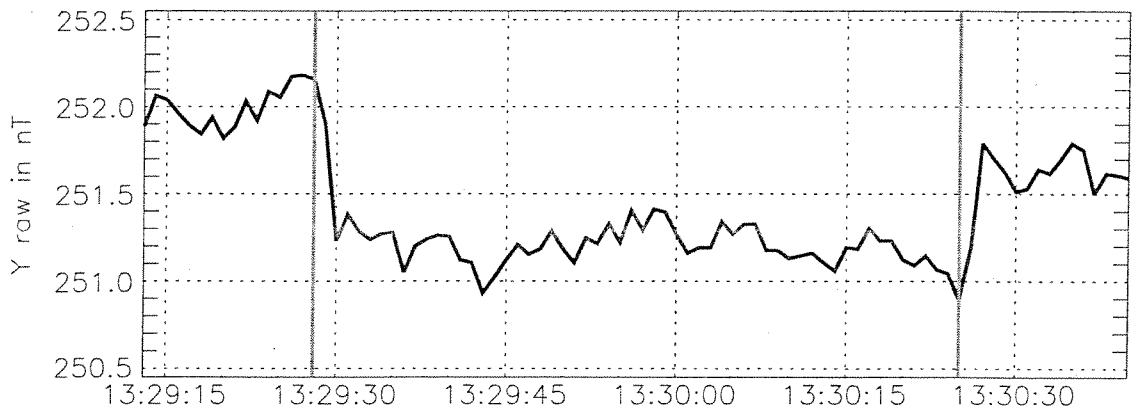


Figure 9-1 Magnetic deflection caused by star cameras, (FGM2 - FGM1)

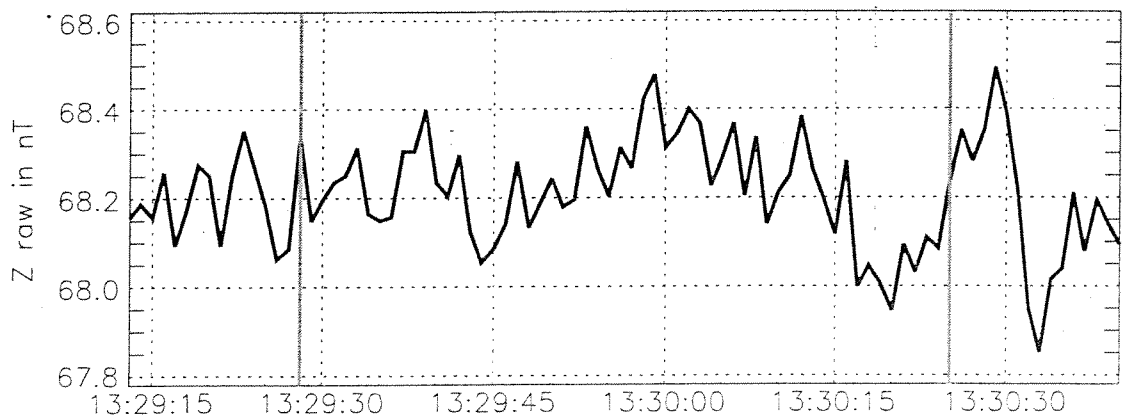
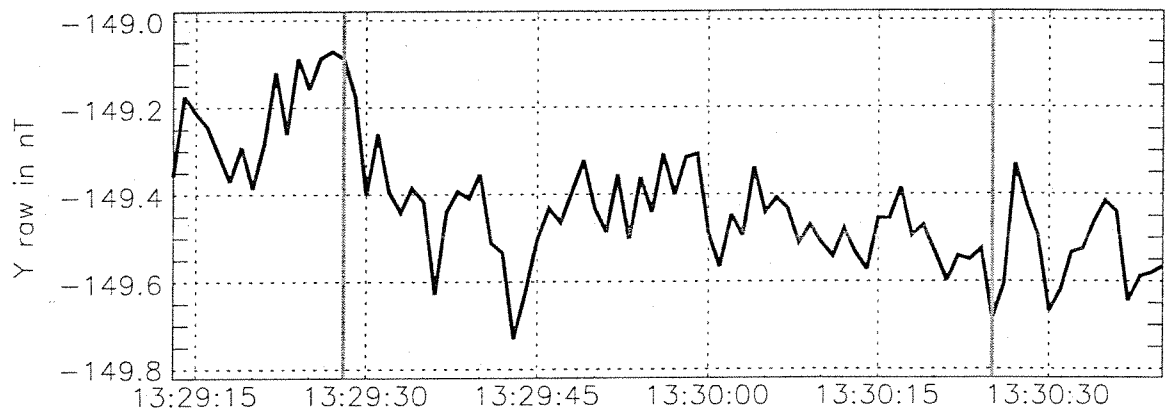
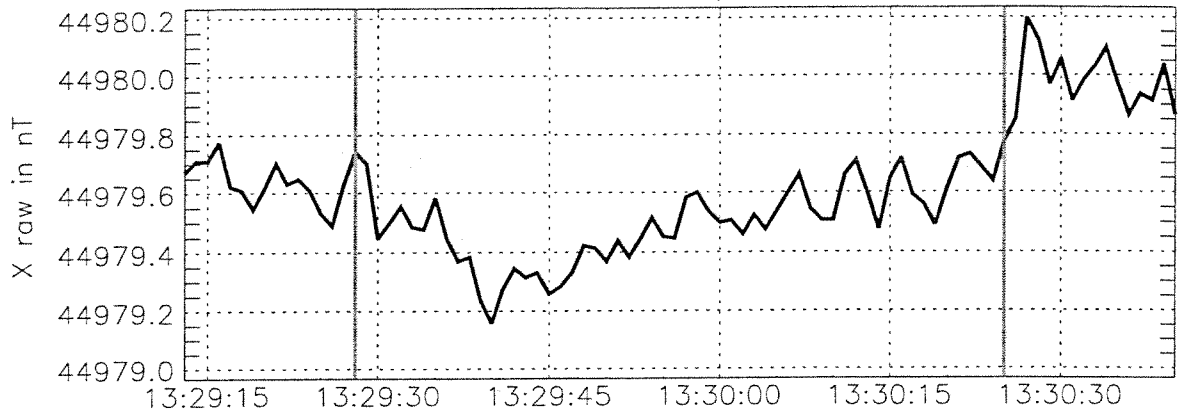
FGM 2 Step 6.12



-c:\p\m2\magcal\15-402000.d\70.Feb.11.13.26.30.1999


Figure 9-2 Magnetic deflection at FGM2 caused by star cameras

FGM 1 Step 6.12



---SAF--- 1 week of 15-MAGS on Thu Feb 11 18:04:47 1998

Figure 9-3 Magnetic deflection at FGM1 caused by star cameras

	Magnetic Calibration Boom Instrumentation Report and Results	Doc: CH-GFZ-TR-2602 Issue: 1.1 Date: 23.5.2000 Page: 43 of 43
---	---	--

10 SUMMARY

The instruments of the CHAMP magnetometry package were calibrated in their flight configuration at the magnetic test facility of the IABG. Due to the stringent requirements imposed by the CHAMP mission objectives a good deal of effort was put in the determination of the facility characteristics and its limitations. As a by-product of this test we can offer detailed numbers on the performance of the facility, e.g. the field gradient in the centre (cf. Figures 6-2 and 6-3) or the temperature coefficient of the scale factors (23 ppm/K).

An important test was the check of the reliability of the scalar calibration. During the CSC calibration in Braunschweig some doubts came up. In a dedicated set of measurements we could reproduce the same result with a scalar calibration using the OVM and a three-tilt calibration using the FGM. The discrepancies encountered in Braunschweig were probably due to the employed GEM scalar magnetometer.

For all the calibration steps characterising the DC features of the FGMs we used the OVM as the reference instrument. This method provided absolute accuracy and circumvented the limitations of the coil facility, but made it necessary to consider the field gradients between the instruments. Despite of this complication the relevant parameters of the FGMs could be determined with an accuracy sufficient for the evaluation of the flight data.

A crucial parameter for a reliable interpretation of the FGM measurements is the temperature of the CSC sensors. Due to a difference in the response characteristic to temperature changes between the thermistors and the feedback coils dedicated tests during the commissioning phase are necessary to ensure an effective dynamic correction of the temperature dependence.

Particularly promising are the results obtained for the angles between the sensor components. No variations could be detected exceeding the measurement uncertainty of 2 arcsec since the first measurements in March 1998. Even the exposure to temperature cycles from -40° to 40° C and a vibration test did not change the numbers. These superior results suggest that we should treat the angles between the components as constant, not handling them as free parameters of the in-flight calibration. This could be advantageous for the reliability of the remaining free parameters.

The noise level of the FGMs was found to be $35 \text{ pT}_{\text{rms}}$. In the full-scale range of $\pm 65000 \text{ nT}$ it represents a resolution of less than 1 ppm. This requires a digitisation depth of about 21 bit. For CHAMP the magnetic field measurements are transmitted as 24 bit values. In the compressed mode the resolution of the digital value is, however, truncated to 20 bit. Experiences during the mission will show which modes are adequate.

Among others, tests of the dynamic behaviour have been used to determine the step response of the FGMs. This feature has to be known, if disturbances from spacecraft subsystems like torquers or thrusters shall be corrected in the data effectively. Furthermore, we could pin down the time which has to be affiliated to a measurement with respect to the time stamp. The obtained precision is 2 ms, for the FGMs in all modes and also for the OVM. The reliable measurement time is a crucial number when deriving quantities which involve readings from different instruments.

Finally we investigated the magnetic disturbances caused by the star sensors on the boom. The camera heads themselves proved to be magnetically very clean. There was neither a remanent nor a soft magnetic effect detected by any of the three magnetometers. Also electric currents in the sensor heads caused only negligible disturbances in the nearby FGM1 sensor CSC1 (0.2 nT when both heads are saturated). Having these great achievements in mind it is disappointing to report that deflections of about 1 nT are caused by the currents through the star camera cables passing by the FGM2 sensor CSC2. In future mission more effort should be put in a better design of the sensor harness ensuring a higher degree of self compensation.

In summary, we may state that we were able to determine all important parameters of the magnetometers with a precision satisfying the CHAMP requirements. The success of this magnetic test is to a good part due to the dedicated support of the facility staff members P. Hertz and R. Lauxen. We are grateful for their cooperation. From the final magnetic test on system level the actual performance of the magnetometry package on board CHAMP will emerge.